GEORGIA DOT RESEARCH PROJECT 18-28

FINAL REPORT

OPTIMIZING WINTER ROADWAY TREATMENTS FOR GEORGIA PAVEMENTS

OFFICE OF PERFORMANCE-BASED MANAGEMENT AND RESEARCH

600 WEST PEACHTREE STREET NW
ATLANTA, GA 30308

TECHNICAL REPORT DOCUMENTATION PAGE

1. Report No.: FHWA-GA-20-1828	2. Government Accession No.: N/A	3. Recipient's Catalog No.: N/A
4. Title and Subtitle: Optimizing Winter Roadway Treatments for Georgia Pavements		5. Report Date: February 2021
		6. Performing Organization Code: N/A
7. Author(s): Junan Shen, Ph.D. (https://orcid.org/0000-0001-6069-4313); Xiaoming Yang, Ph.D. P.E. (https://orcid.org/0000-0002-6308-0912); Youngguk Seo, Ph.D. (https://orcid.org/0000-0002-6495-2153); and Tien Yee, Ph.D.		8. Performing Organization Report No.: 18-28
9. Performing Organization Name and Address: Georgia Southern University 201 COBA Drive, Building 232 Statesboro, GA 30460-8077 Phone: (912) 478-0084 Email: jshen@georgiasouthern.edu		10. Work Unit No.: N/A
		11. Contract or Grant No.: PI#0016893
12. Sponsoring Agency Name and Address: Georgia Department of Transportation Office of Performance-based Management and Research 600 West Peachtree Street NW Atlanta, GA 30308		13. Type of Report and Period Covered: Final; Sep 2019 – Feb 2021
		14. Sponsoring Agency Code: N/A
15. Supplementary Notes: Prepared in cooperation with the U.S. Department of Transportation, Federal Highway Administration.		

16. Abstract:

The purpose of this project is to optimize the current practice of winter roadway treatments in Georgia by evaluating the efficiency of deicers commonly used by GDOT (i.e., sodium chloride and calcium chloride) on deicing and anti-icing and the effects of these deicers on pavement materials. To this end, the freezing point, penetration capability, ice and snow melting capacity were investigated on five different combinations of deicers, i.e., a fixed 23% NaCl plus one of five various $CaCl_2$ contents of 0, 10, 15, 20, and 25%. The effects of the brines of the deicers on asphalt binders were evaluated by comparing the performance properties of the asphalt binders before and after soaking in the five brines for 7 and 28 days. The effects of the brines on the Portland cement concrete (PCC) and steel were evaluated on the strength of PCC cylinder samples after the samples were subjected to freeze–thaw (F–T) cycles in the brines and the surface conductivities. The results of the tests indicated, first, that the dose of $CaCl_2$ lowered the freezing points quickly for a low dose up to 15 percent and slowly for 15–25 percent. The capability of brine penetration on ice depended on the temperature of the ice and the dose of $CaCl_2$. There was no penetration at all when ice was at 5°F. The melting capacity of solid deicers on the ice and snow was consistent with the penetration capacity of the brines. Second, the changes in the performances of the $G^*/\sin(\delta)$, $G^*\sin(\delta)$ and stiffness, and m-value of asphalt binders when soaked varied with type of binder and dose of CaCl2, although most of the changes were positive. A statistical analysis of variance (ANOVA) indicated that these changes were insignificant for the doses of $CaCl_2$, but unmodified asphalt binders caused significant changes as compared with the modified asphalt binders. Third, increased dose of $CaCl_2$ caused more damage on PPC cylinders, but a low dose of $CaCl_2$ caused more F–T damage. A recommended material selection and application rate guideline is also provided.

17. Keywords: Anti-icing, Deicing, Pavement, Maintenance	18. Distribution Statement: No Restriction

19. Security Classification (of this report): Unclassified	20. Security Classification (of this page): Unclassified	21. No. of Pages: 123	22. Price: Free

GDOT Research Project No. 18-28

Final Report

OPTIMIZING WINTER ROADWAY TREATMENTS FOR GEORGIA PAVEMENTS

By
Junan Shen, Georgia Southern University
Professor

Xiaoming Yang, Georgia Southern University
Assistant Professor

Youngguk Seo, Kennesaw State University
Associate Professor

Tien Yee, Kennesaw State University
Associate Professor

Georgia Southern University Research and Service Foundation, Inc.

Contract with
Georgia Department of Transportation

In cooperation with
U.S. Department of Transportation
Federal Highway Administration

February 2021

SI* (MODERN METRIC) CONVERSION FACTORS

APPROXIMATE CONVERSIONS TO SI UNITS

Symbol	When You Know	Multiply By	To Find	Symbol
		LENGTH		
in	inches	25.4	millimeters	mm
ft	feet	0.305	meters	m
yd	yards	0.914	meters	m
mi	miles	1.61	kilometers	km
		AREA		
in^2	square inches	645.2	square millimeters	mm^2
ft^2	square feet	0.093	square meters	m^2
yd^2	square yard	0.836	square meters	m^2
ac	acres	0.405	hectares	ha
mi^2	square miles	2.59	square kilometers	km^2
		VOLUME		
fl oz	fluid ounces	29.57	milliliters	mL
gal	gallons	3.785	liters	L
ft^3	cubic feet	0.028	cubic meters	m^3
yd^3	cubic yards	0.765	cubic meters	m^3
		NOTE: volumes greater than 1000 L shall be shown in m^3		
		MASS		
oz	ounces	28.35	grams	g
lb	pounds	0.454	kilograms	kg
T	short tons (2000 lb)	0.907	megagrams (or "metric ton")	Mg (or "t")
		TEMPERATURE (exact degrees)		
^oF	Fahrenheit	5 (F-32)/9 or (F-32)/1.8	Celsius	^oC
		ILLUMINATION		
fc	foot-candles	10.76	lux	lx
fl	foot-Lamberts	3.426	candela/m^2	cd/m^2
		FORCE and PRESSURE or STRESS		
lbf	poundforce	4.45	newtons	N
lbf/in^2	poundforce per square inch	6.89	kilopascals	kPa

APPROXIMATE CONVERSIONS FROM SI UNITS

Symbol	When You Know	Multiply By	To Find	Symbol
		LENGTH		
mm	millimeters	0.039	inches	in
m	meters	3.28	feet	ft
m	meters	1.09	yards	yd
km	kilometers	0.621	miles	mi
		AREA		
mm^2	square millimeters	0.0016	square inches	in^2
m^2	square meters	10.764	square feet	ft^2
m^2	square meters	1.195	square yards	yd^2
ha	hectares	2.47	acres	ac
km^2	square kilometers	0.386	square miles	mi^2
		VOLUME		
mL	milliliters	0.034	fluid ounces	fl oz
L	liters	0.264	gallons	gal
m^3	cubic meters	35.314	cubic feet	ft^3
m^3	cubic meters	1.307	cubic yards	yd^3
		MASS		
g	grams	0.035	ounces	oz
kg	kilograms	2.202	pounds	lb
Mg (or "t")	megagrams (or "metric ton")	1.103	short tons (2000 lb)	T
		TEMPERATURE (exact degrees)		
^oC	Celsius	1.8C+32	Fahrenheit	^oF
		ILLUMINATION		
lx	lux	0.0929	foot-candles	fc
cd/m^2	candela/m^2	0.2919	foot-Lamberts	fl
		FORCE and PRESSURE or STRESS		
N	newtons	0.225	poundforce	lbf
kPa	kilopascals	0.145	poundforce per square inch	lbf/in^2

* SI is the symbol for the International System of Units. Appropriate rounding should be made to comply with Section 4 of ASTM E380. (Revised March 2003)

TABLE OF CONTENTS

LIST OF FIGURES

LIST OF TABLES

EXECUTIVE SUMMARY

BACKGROUND

During the winter, operations to reduce the effects of ice and snow on the pavement are crucial to highway safety, including those executed before, during, and after a winter weather event such as snow. GDOT currently uses a variety of winter treatments, including salt brine, rock salt, granular calcium chloride, and abrasives (89 stone). The selection of winter treatment strategy is largely based on the weather condition and the availability of materials. In recent years, it has been recognized nationwide that the use of anti-icing and deicing chemicals may accelerate the deterioration of roadway pavements. The impact depends on the type of chemical(s) used and the dosage. Therefore, a need exists to evaluate the efficiency and further optimize the current practice of winter roadway treatments in Georgia to produce a safe and long-lasting transportation infrastructure.

OBJECTIVES

This research aims to optimize the winter treatment operations in Georgia and specially to minimize the impact to Georgia pavements. Both anti-icing and deicing operations will be considered in the research. The objectives of this research are to: (1) examine the effectiveness of commonly used ice-control chemicals in Georgia at different dosages; (2) evaluate the deterioration of the pavement surface course caused by commonly used ice-control chemicals; and (3) propose to GDOT practical and optimum solutions for anti-icing/deicing.

FINDINGS

1. The 23% NaCl brine prepared with the GDOT rock salt had a measured freezing point of 3.2°F (−16°C). The freezing point of the brine decreased when additional calcium chloride was added into the 23% NaCl brine. The measured freezing point of the blended brine ranged from 2.2°F (−19°C) with 5% CaCl2 to 20.2°F (−29°C) with 25% $CaCl_2$. In general, the measured freezing points from GDOT salts were slightly higher than the pure salt brines due to the impurity of the GDOT salts.
2. The measured freezing points of blended salt brines were slightly different from the calculated values from the theoretical equation. A regression equation was calibrated from the test data, which can be used to calculate the freezing point of blended brines prepared with GDOT salts.
3. Blended brines of calcium and sodium chlorides demonstrated some capacity to penetrate ice (for deicing) at 25.0°F (−3.9°C) temperature. The capacity decreased quickly with decrease in temperature and showed very limited penetration to the ice at temperatures of 15°F and below.
4. Blended solid deicers of sodium and calcium chlorides were more effective and economical than using rock salt alone when the temperature was below 2.0°F (−16.7°C). As the temperature increased, there existed an optimum blend ratio of calcium chloride to achieve the lowest material cost. When the temperature was above 20.0°F (−6.7°C), it was not necessary to use calcium chloride in the solid deicer, as it increased the material cost. At medium temperatures of 2.0°F (−16.7°C) to 20.0°F (−6.7°C), the optimum mixing ratio of calcium chloride was around 0.05 to 0.15 per part of sodium chloride.

5. The retention rate of the brine on the road surface depends on the pavement smoothness. The measured retention rate from OGFC (open-graded asphalt friction course), Superpave (SUperior PERforming Asphalt PAVEments), and PCC (Portland cement concrete) pavements were 97, 92, and 77 percent, respectively. The retention rate reduced when the grade of the pavement surface exceeded 10 percent; however, the effect was negligible when the surface grade was less than 10 percent. Further, the retention rate of the brine was higher on dry pavements than on wet pavements.
6. The rheological property at high temperatures, $G^*/\sin(\delta)$, of original binders and rolling thin film oven (RTFO) residuals after soaking were observed to increase slightly regardless of the duration of soaking, indicating the rutting resistance of the tested binders was not negatively affected by soaking. There was a significant difference of $G^*/\sin(\delta)$ caused by the type of binder, i.e., the unmodified binders were more sensitive to soaking in brines.
7. The $G^*\sin(\delta)$ at intermediate temperatures was generally slightly increased after being soaked in a brine of 23% NaCl, and then decreased with the continued addition of $CaCl_2$. The differences of increase and decrease in $G^*\sin(\delta)$ were, however, insignificant with regard to the type of binder and the dose of calcium chloride. This result indicates a mixed effect of brines on the fatigue performance of the binders.
8. The soaking of all the asphalt binders in a 23% NaCl brine caused, in general, a decrease in the stiffnesses, and an increase in the m-values indicated some degree of improvement of the low-temperature properties. The effect of the dose of

calcium chloride, in general, decreased the stiffnesses and increased slightly the m-values of the asphalt binders, which, again, improved their low-temperature properties. Both the creep properties of stiffness and m-value have significant differences caused by the type of binder.

9. Given the range of brine concentrations, higher concentrations (20% and 25% CaCl2) caused more damage in PCC pavement than lower concentrations (0%, 5%, and 10% CaCl2) when concrete is constantly exposed to brine solutions at above-freezing temperatures. On the other hand, concrete samples appeared more prone to freeze-thaw (F–T) damages at lower concentrations (0% and 5% $CaCl_2$), which is also confirmed with surface scaling and weight loss data.
10. Soaking of asphalt binders in solutions of deicers decreased the Young's modulus and adhesion force regardless of the type of asphalt binders. Furthermore, both Young's modulus and adhesion decreased as the dose of deicers in the solution increased.
11. The epoxy-coated (EC) dowel bars were found to be excellent in preventing any corrosion. Type F fly ash would be effective in reducing F–T damage across the brine concentrations. This favorable effect was further escalated in ambient erosion conditions, especially at 0% $CaCl_2$. At above-freezing temperatures, a slightly higher air content than 6.5% was beneficial for PCC pavement to be resistant to chloride ions, especially at lower concentrations (0% and 5% $CaCl_2$), but air contents too high (12% in this study) would show no benefits.

CHAPTER 1. INTRODUCTION

BACKGROUND

Anti-icing and deicing are important roadway treatment procedures to maintain the highway traffic safety during winter seasons. Anti-icing refers to proactive procedures that prevent ice from forming or bonding to the road surface. Deicing refers to post-treatment procedures that help to clear the snow or ice cumulated on the road surface. Both anti-icing and deicing treatments involve the application of salt chemicals in either liquid or solid forms. Due to the complex nature of ice forming and melting, the timing and the rate of the salt application are important decisions to make by highway transportation agencies.

Although Georgia is in a relatively mild winter climate zone, winter weather events may occur in northern districts, which can potentially cause significant congestion and safety issues especially in the Atlanta metropolitan area. Georgia Department of Transportation (GDOT) has been using salt chemicals to fight snow and ice on high-volume interstate routes for years. The current procedure of roadway treatment has been working effectively in controlling snow and ice. Recently, however, pre-mature pavement distresses have been observed on some winter roadway treatment routes, which raised some concerns on the possible adverse effect of the salt application. Therefore, an evaluation of the current GDOT winter roadway treatment procedures, especially on the salt types and application dosages, is needed.

OBJECTIVE

This research aims to optimize the winter treatment operations and specially to minimize the impact to Georgia pavements. Both anti-icing and deicing operations are considered in the research. The objectives of this research are to: (1) examine the effectiveness of commonly used ice-control chemicals in Georgia at different dosages; (2) evaluate the deterioration of pavement surface course caused by commonly used ice-control chemicals; and (3) propose to GDOT practical and optimum solutions for anti-icing/deicing.

LITERATURE REVIEW

The research team reviewed existing publications in the following three areas: (1) winter roadway treatment guidelines; (2) the current practice in other state DOTs; (3) the effectiveness and adverse effects of common salt chemicals.

Winter Roadway Treatment Guidelines

The American Association of State Highway and Transportation Officials (AASHTO) published a guideline on the use of anti-icing and de-icing materials in 2004.[1] This document outlined a decision-making procedure for the salt application based on road and weather conditions. The effective temperature and the application rate of five typical salt chemicals were also provided based on theoretical analyses. An update to the AASHTO guideline was published in 2008 to address some new equipment, materials, and technologies.[2] It has also been recognized that anti-icing operation plays an important role in an efficient winter roadway maintenance. Federal Highway Administrations (FHWA) published a practice manual for anti-icing operations.[3] The manual includes a decision-

making toolbox which covers the selection and the application of four common salt chemicals.

Current Practice in State DOTs

Many state DOTs have developed their own winter roadway treatment guidelines. These guidelines largely follow the federal publications described in the previous section. However, the type of salt chemical, the form of application (solid, pre-wetted solid, or liquid), and the application rate vary from state to state. The research team has reviewed published guidelines from 22 states with a focus on the salt application practice. The findings from the literature review are summarized as follows.

Sodium chloride (NaCl) and calcium chloride ($CaCl_2$) are the two most used salt chemicals for snow and ice control. Other less commonly used salt chemicals include magnesium chloride, potassium acetate, potassium formate, calcium magnesium acetate, sodium acetate, and sodium formate.

For anti-icing, many states prefer to use liquid application (brine) when the whenever weather and road conditions allow. Usually, 23% of NaCl brine is the default when the pavement is dry and the temperature at the onset of the winter weather event is higher than 15~20°F. The application rate of the NaCl brine varies from 10~90 gal/lane-mile depending on the weather event with the most common rate of 30~40 gal/lane-mile. Some states apply 30~32% $CaCl_2$ brine at a rate of 15~70 gal/lane-mile for anti-icing when the temperature is too low for the NaCl brine to work.

Solid and prewetted applications can be used for deicing and sometimes for anti-icing operations when the weather and road conditions prohibit a liquid application. Coarse-graded salt is generally more cost-effective than fine-graded salt. Salt with a fine grade is not ideal for deicing because it has a high potential of dilution. For anti-icing, the application rate for NaCl (rock salt) ranges from 75 to 400 lb/lane-mile in different states. Solid salt can be prewetted with sodium (and sometimes calcium and magnesium) chloride solutions before application. Prewetting enhances the performance of solid salt as it helps the solid salt to adhere to the road surface.

Adverse Effects of Common Salt Chemicals

Overall, the amount of salts used in Georgia for anti-icing and deicing is much less than some northern states of the country where the adverse effects of the salt chemicals have been a bigger concern. The adverse effects of roadway treatment using salts can be categorized into operational, environmental, and infrastructural impacts. The operational impact refers to the potential slick condition caused by the anti-icing salt chemicals on the road surface. The slick condition usually occurs when the when the road temperature is above 40°F and the relative humidity is around 30~40%. Washington DOT's *Snow and Ice Plan* provides general guidelines to mitigate this adverse effect.[4] Excess amount of chlorides deicers may leach into the environment through runoff water. A NCHRP synthesis report discussed strategies to mitigate the environmental impact of deicers.[5] In this study, the literature review focused on the infrastructural impact of salt chemicals on asphalt and concrete pavements.

Asphalt pavements are surfaced with asphalt concrete. Asphalt concrete is a mixture of asphalt binder and aggregate. The deterioration of asphalt concrete may occur through aging of asphalt binder, weathering of aggregate particles, and loss of adhesion between the two ingredients. Overall, very few research studies were conducted in this area. A group of researchers in Canada tested both aggregate and asphalt concrete mixture samples (cored from field) subjected to freeze–thaw (F–T) and liquid deicers.[6] After 30 F–T cycles, aggregate samples immersed in four deicer solutions (including NaCl) all lost more weight than the control samples (immersed in distilled water), which indicated a loss of durability due to the deicers. The F–T test on asphalt concrete samples did not show significant effect on durability due to deicers except for samples immersed in urea. However, it should be noted that the concentration of deicer solutions used to condition the asphalt concrete samples in this research was only 2% of saturation concentration.

Chlorides affect the durability of Portland Cement Concrete (PCC) pavements both physically and chemically. Physical effects result in cracking and surface scaling. Several mechanisms have been identified to explain the phenomenon of surface scaling, including thermal shock, growth of salt crystals, hydraulic pressure, and glue spalling.[7-9] Chemical effects of chlorides on PCC can result from reactions involving cement hydration products, aggregates, or reinforcing steel. Reactions caused by chloride ions in brine include the leaching of calcium hydroxide from the paste, the decalcification of calcium silicate hydrate (C-S-H), the conversion of C-S-H to magnesium silicate hydrate (M-S-H), and the formation of brucite, complex salts, and oxychlorides. The alkali-silica reaction and alkali-carbonate reactions can be initiated and accelerated by alkalis from deicers. The

accumulation of chloride ions in the vicinity of the steel, such as dowel bars in pavement joints, can induce corrosion when specific temperature and humidity conditions are met.[10]

RESEARCH SCOPE

In this study, all materials and specimens used in the laboratory test were collected locally in Georgia or prepared according to GDOT standards. In order to achieve the research objectives outlined earlier in this chapter, the experimental work focused on three areas. First, physical and engineering properties of GDOT salt samples were tested. The test results and analysis are presented in Chapter 2 of this report. Second, properties of typical Georgia asphalt binders were measured with and without exposure to brine solutions. The test results and analysis are presented in Chapter 3 of this report. Last, the impact of brine solutions on PCC and reinforcement were evaluated. This part of study was conducted in the material laboratory at Kennesaw State University, and the results and analysis are presented in Chapter 4.

CHAPTER 2. SELECTED PHYSICAL AND ENGINEERING PROPERTIES OF GDOT SALTS

This chapter examines the freezing and ice melting properties of deicers currently used by GDOT. The focus is on blended mixes of sodium and calcium chlorides at different ratios. Both brines and solid deicers were tested in the laboratory. The material properties evaluated included: (1) the freezing point of brines, (2) the ice penetration rate of brine, (3) the ice melting capacity of granular deicers, and (4) the snow melting capacity of solid deicers. In addition, the retention rates of brines on asphalt and concrete pavement surfaces were investigated.

MATERIALS

The sodium chloride (figure 1-A) used in the study was sampled from one of the GDOT salt storage facilities near Atlanta, Georgia. The chemical properties of the material, such as purity, are unknown. The sample consists of angular, well graded salt particles. The sodium chloride sample was crushed with a rubber mallet and passed through a No. 4 standard sieve before further testing. Screening the sample helps to reduce the variation of the laboratory test result when only a small amount of material is used in each test.

The calcium chloride (figure 1-B) sample in this study is from a commercial product provided by District 5 of Georgia. The material properties are listed in table 1. The sample was taken from the original package and then stored in a sealed container to avoid absorption of water from the air. The calcium chloride sample consists of rounded, poorly graded pellets with a nominal maximum size of about 1/8 inch (3.2 mm). Due to the

uniformity of the material, the calcium chloride sample was directly used in the test without crushing or screening.

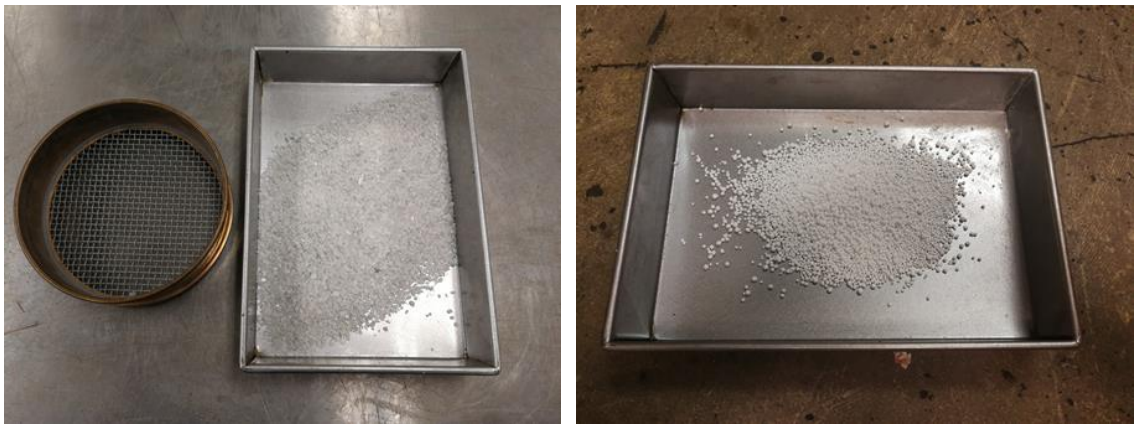

(A) GDOT sodium chloride (B) GDOT calcium chloride

Figure 1. Photos. Sodium chloride and calcium chloride samples.

Table 1. Properties of the GDOT calcium chloride.

Characteristics	**Typical Value***
Calcium chloride assay	>90.0%
Pellet size distribution >4.8 mm 0.6–4.8 mm <0.6 mm	 <20.0% >76.0% 4.0%
Bulk density	58–66 lb/ft^3
ASTM D98 Purity Requirement** Total alkali chlorides (as NaCl) Total magnesium (as $MgCl_2$) Calcium hydroxide	 <6.0% <0.5% >0.2%

* All properties are by weight
** On an active ingredient basis

The raw materials of sodium and calcium chlorides were used to make different blends of brines and deicing solids. The blend ratios are listed in table 2. Pictures of the brine

(Samples B-1 to B-5) and solid blends (Samples D-1 to D-5) are presented in figure 2-a and figure 2-b, respectively.

Table 2. Ratios of the blended mixes.

Brine	Sodium Chloride (%)	Calcium Chloride (%)
B-1 and D-1	23	0
B-2 and D-2	23	10
B-3 and D-3	23	15
B-4 and D-4	23	20
B-5 and D-5	23	25

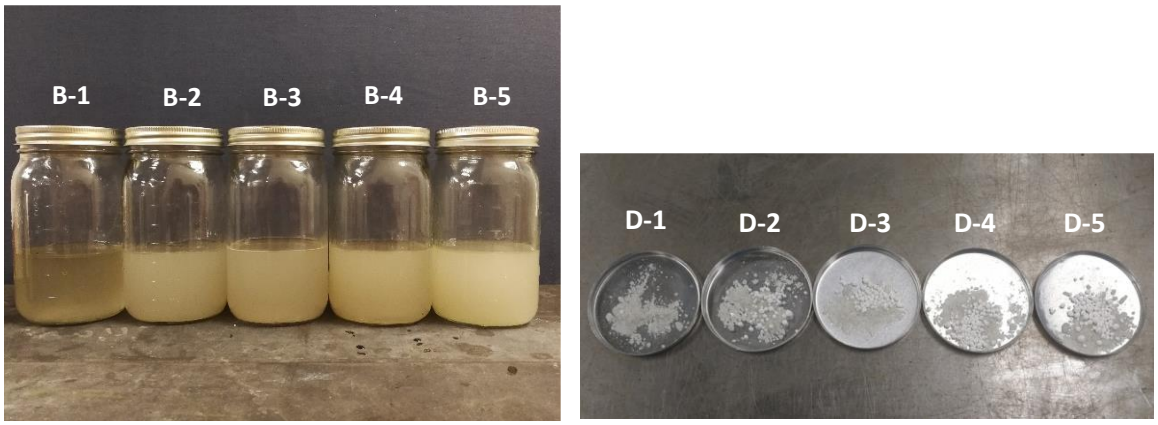

(a) Blended mixes of brines (b) Blended mixes of solid

Figure 2. Photos. Brines and solid deicers at different blend ratios.

FREEZING POINTS OF BRINES

The freezing point is the temperature of the brines at which crystallization begins in the absence of supercooling or, in the case of supercooling, the maximum temperature reached immediately after initial crystal formation. The freezing point test used in the study is standardized by ASTM D1177.[11]

Freezing Point Test Device and Procedure

Figure 3 shows the freezing point test device assembled in-house. In this test, about 50 g of brine sample were cooled in a cold bath (i.e., a mixture of dry ice and denatured alcohol). A motor-driven stirrer was used to ensure a uniform temperature change in the brine sample. The temperature of the brine was recorded continuously until the brine became frozen, and the "turning point" after supercooling on the temperature–time curve was taken as the freezing point.

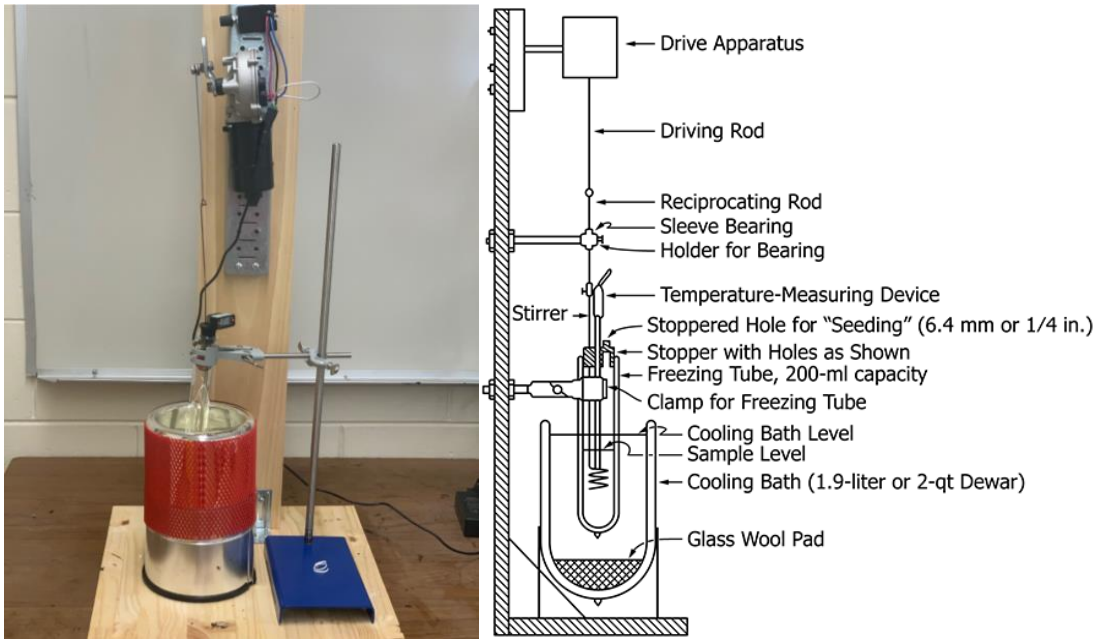

Figure 3. Photo and illustration. Freezing point test device.

Freezing Point Test Result

Figure 4 shows the curves of the freezing points and measured time of the five brines, i.e., B-1 to B-5. The baseline brine with 23% NaCl (Sample B-1) showed a much higher freezing point than those of the other four brines with blended calcium chloride of different

percentages (Samples B-2 through B-5). The blended brines also took a longer time to reach their freezing points compared to the baseline brine (B-1). This result demonstrated the effectiveness of calcium chlorides in lowering the freezing points; however, further increase in the calcium content in the brine beyond 10 percent became less effective in reducing the freezing point. It should be noted that the concentration of brine here is not the same as the concentration of brine on the road during the winter precipitation event, because brine is simply a way to deliver the salt onto the pavement. However, the result does indicate in a sense that there may be an optimum amount of calcium content depending on the temperature and the amount of precipitation during the event.

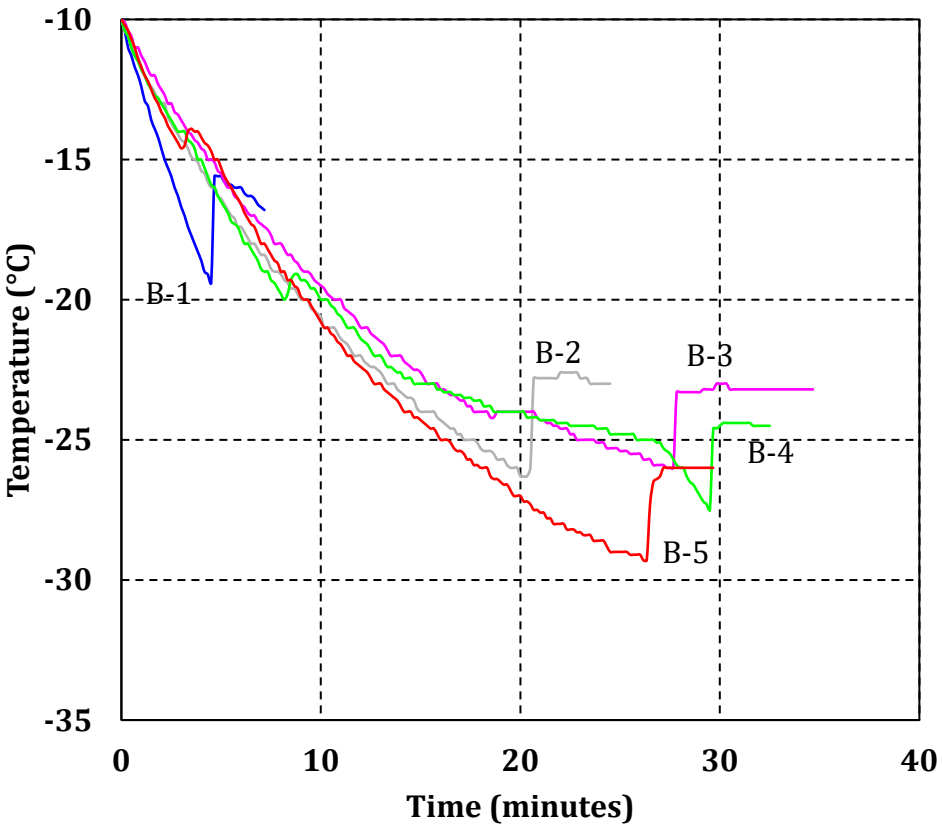

Figure 4. Graph. Freezing point test curves.

For comparison, brines were also prepared with pure sodium and calcium chlorides at the same blend ratios as Samples B-1 to B-5 and an additional ratio of 23% NaCl + 5% $CaCl_2$. The freezing points of these pure salt brines were tested and are compared with GDOT salt brines in figure 5. Overall, the freezing points of the GDOT salt brines were slightly higher than that of the pure salt brines, with a less than 3°F difference. This difference is likely due to the impurity of the GDOT salts.

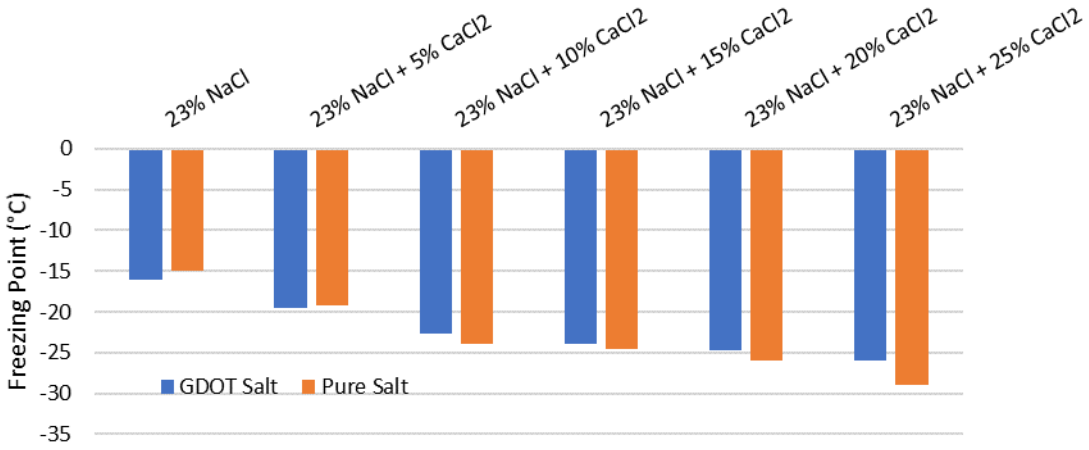

Figure 5. Graph. Freezing points of GDOT salt brines and pure salt brines.

The slope of the freezing point test curve indicated the average rate of freezing during the test. Figure 6 compares the average rates of freezing measured from the GDOT brines and the pure salt brines. In general, the measured freezing points increased as the concentration of both GDOT and pure salts increased within the concentration limit of 20 percent in this study. When the concentration of deicers was higher than the limit discussed, the general trends were not true. The pure salts on the other hand had an increasing slope for GDOT samples but a decreasing slope for pure samples as the concentration of salts increased.

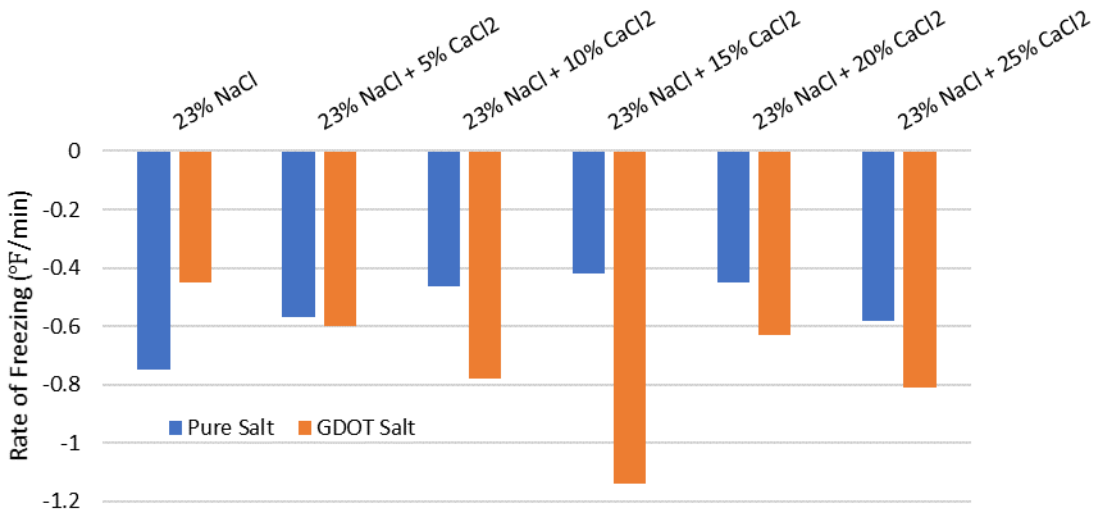

Figure 6. Graph. Average rate of freezing of GDOT salt brines and pure salt brines.

Comparison Between Measured and Calculated Freezing Points

Freezing points can be calculated using the weight of deicers present in saturated aqueous faces. This consists of the molecular concentration of the deicer material and can be expressed as the molecular weights of the material in 1000 g of water. It is more accurate for lower concentration. The formula can be written as equation (1):

$$AT = k*C = 1.86C \quad (1)$$

Where,

T = freezing point depression in °C

k = freezing point depression constant (-1.86 for water)

C = deicer concentration (equivalent weight basis) in equivalents per 1000 g water

The calculated freezing points from this theoretic equation were plotted and compared to the experimental data. According to

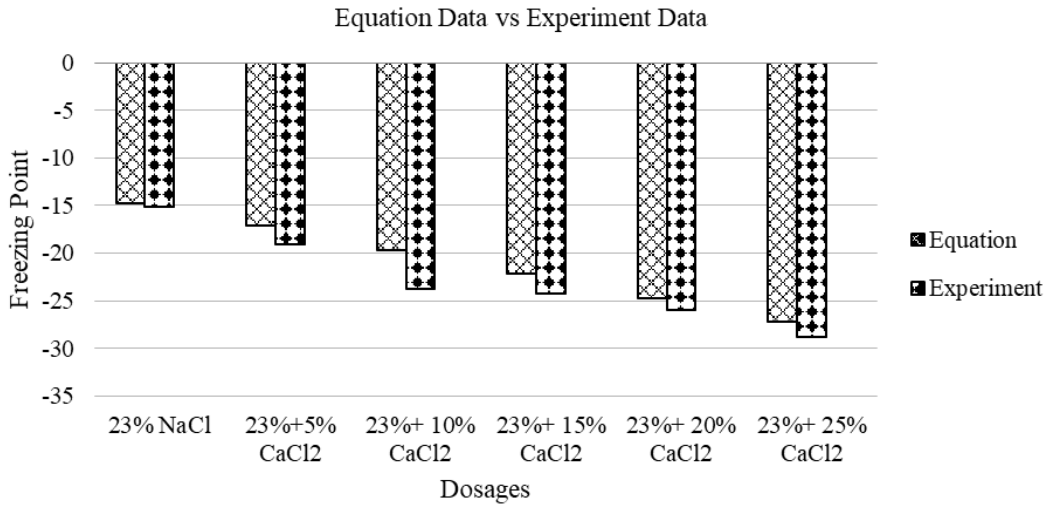

figure 7, the experimental data had a lower freezing point than those from the equation. The percent difference between the calculated and the experimental freezing point was calculated. All the data had a percentage difference of less than 15 percent except the 23% NaCl + 10% $CaCl_2$, which had the highest percent difference of 17.11 percent. The lowest difference was calculated on the solution of 23%. Data of the percent error are listed in table 3.

Table 3. Difference between measured and calculated freezing point with variation of $CaCl_2$.

Brine Dosages	23% NaCl	23% NaCl + 5% $CaCl_2$	23% NaCl+ 10% $CaCl_2$	23% NaCl+ 15% $CaCl_2$	23% NaCl + 20% $CaCl_2$	23% NaCl+ 25% $CaCl_2$
Percent Difference (%)	2.83	10.21	17.11	8.35	4.89	5.52

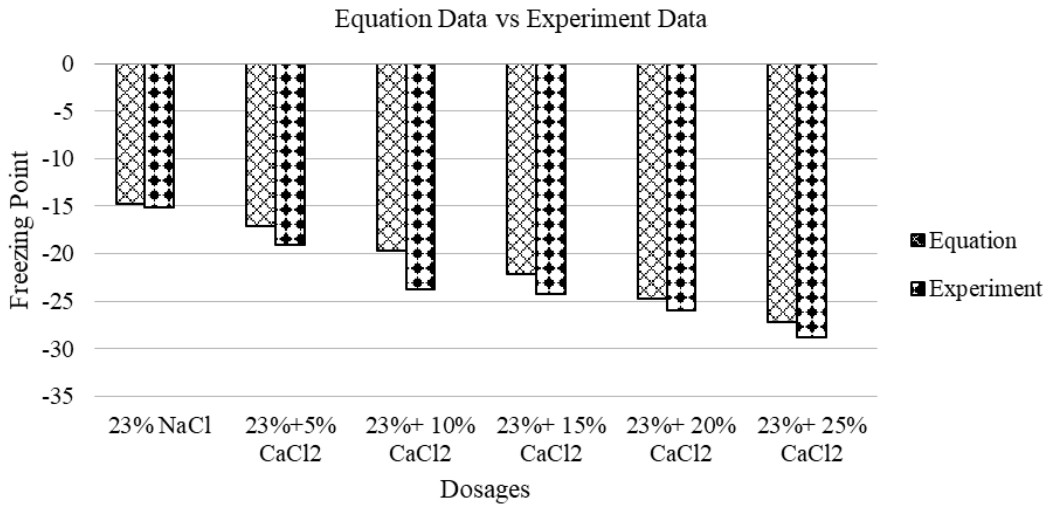

Figure 7. Graph. Experimental and calculated freezing points.

ICE PENETRATION TEST

Deicing (or posttreatment) is occasionally carried out with brines. The ice penetration rate is a measurement of the effectiveness of brines in deicing. The ice penetration test used in this study is standardized in SHRP H 205.4.[12]

Ice Penetration Test Device and Procedure

The test device for the ice penetration test is shown in figure 8. The ice penetration test was performed in a freezer and repeated at various temperatures from −5°F~25°F (−31°C~−4°C). For this test, an ice holder apparatus was fabricated using clear acrylic sheets with holes of 15-5/32 inch diameter drilled into it. Vertical ice tubes were prepared by freezing water in the holes at the test temperature. During the test, about 30 µL of liquid brine sample colored with a blue dye were applied to the top surface of each ice tube. For each brine sample tested, five ice tubes were used. The average brine penetration depth

was taken with image analysis; photo images of the ice holder were taken periodically at 5, 10, 15, 20, 30, and 60 minutes.

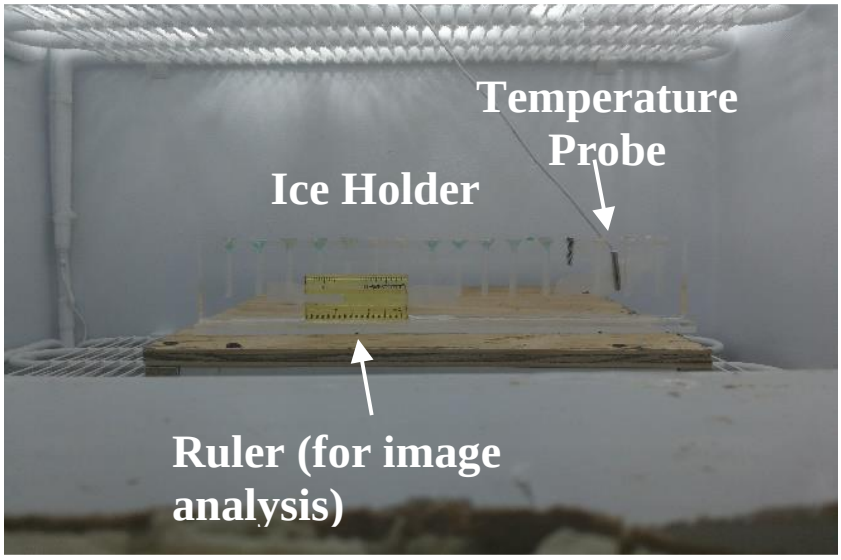

Figure 8. Photo. Ice penetration test device.

Ice Penetration Rate of Brines

The ice penetration test result on the five brine samples is presented in table 4. Overall, the measured ice penetration depth (@ 1 hr) increased with the calcium chloride content at 25°F (−4°C). When the temperature dropped to 15°F and below, even the blended brines with high calcium contents (Samples B-4 and B-5) showed very limited ice penetration in 1 hour. The reduced penetration depth from Sample B-5 at 25°F (−4°C) may have been caused by the undissolved salt that was not able to be collected from the sample container by syringe. The dissolution issue with higher calcium chloride content samples was explained previously.

Table 4. Ice penetration test result.

Brine Sample	Average Penetration Depth @ 1 hr (mm)		
	25°F	15°F	5°F
B-1	0.88	N	N
B-2	1.08	N	N
B-3	2.22	N	N
B-4	2.80	0.1	N
B-5	2.36	0.1	N

Note: N = Negligible penetration

ICE MELTING TEST

Ice melting capacity measures the weight of ice melted by the solid deicers in 1 hour. It is a performance test of solid deicers.

Ice Melting Test Device and Procedure

The ice melting test was, again, conducted in a freezer and repeated at various temperatures from −5°F~25°F (or −31°C~−4°C). Two temperature probes were used during the test to measure the temperature both inside and outside of the ice. This was to ensure the temperature in the ice sample was in equilibrium with the ambient temperature in the freezer. The test setups for the ice penetration test and the ice melting test are presented in figure 9.

Figure 2-B shows the five blended solid deicers of D-1 to D-5 in aluminum discs of 2.5-inch diameter. The deicers were covered and placed in the freezer at least 2 hours before the test to allow them to reach equilibrium to the test temperature.

The ice melting test (SHRP H 205.1) was conducted by solid deicers. In this test, a thin layer of ice was prepared with 60 g of water in a disc 6-inch in diameter at each testing temperature. The disc was covered during the freezing process to produce an even and smooth ice surface. The thickness of the ice produced in this way was about 1/8-inch. During the test, solid deicers were placed on top of the ice sheet. The weight of ice melted is determined by pouring out the melted brine to a container, measuring the weight, and then pouring it back onto the ice sheet. This measuring process was repeated every 10 minutes up to 1 hour.

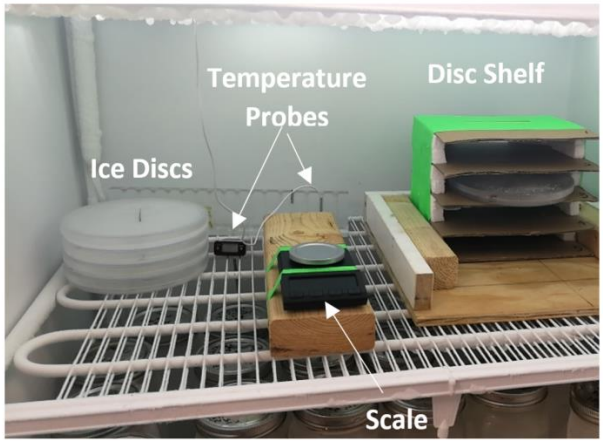

Figure 9. Photo. Ice melting device.

Ice Melting Capacity of Solid Deicers

Figure 10 shows the ice melting test results for the solid deicer samples of D-1 through D-5. The test was repeated at four different target temperatures (25°F, 15°F, 5°F, and −5°F). Due to the test operation and the limitation of the equipment, the actual test temperatures in the freezer varied from the target ones to some extent. The actual test temperatures in the four tests are indicated in each subpart in figure 10.

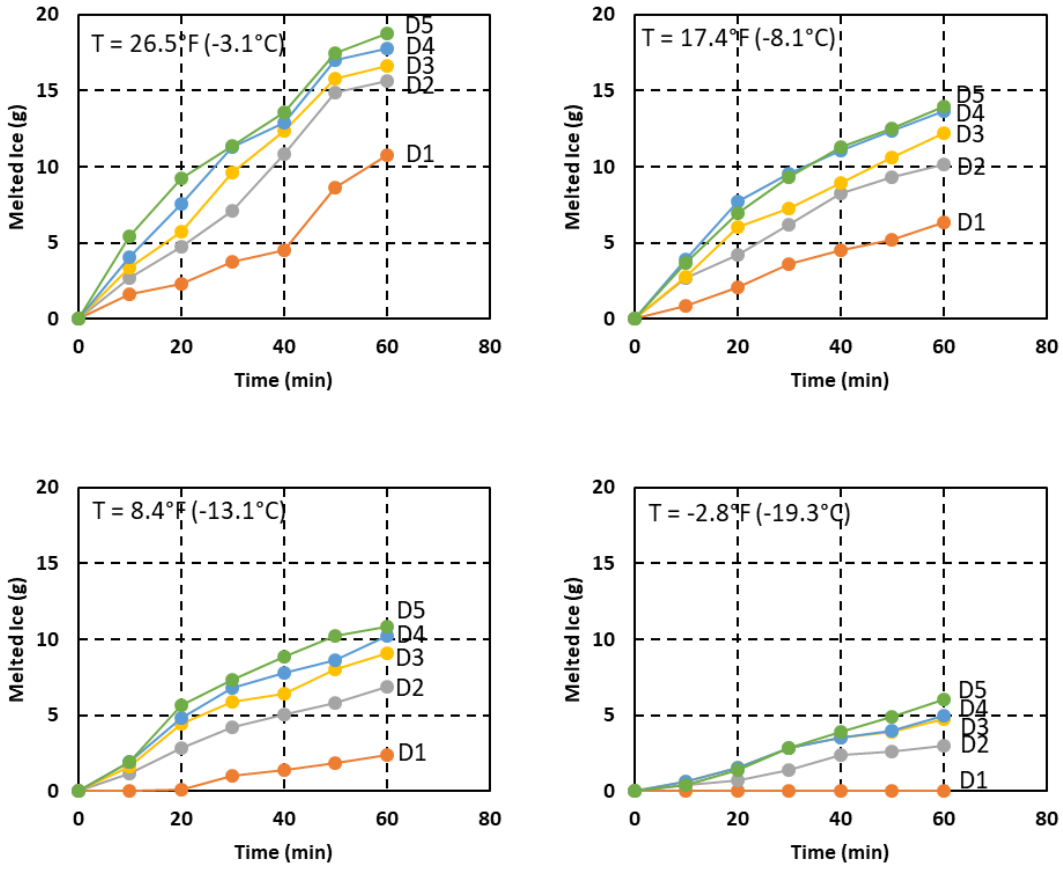

Figure 10. Graphs. Ice melting test results from different blended solid deicers.

The ice melting test results show that sodium chloride has very limited ice melting capacity at 8.4°F (−13.1°C) and almost zero ice melting capacity at −2.8°F (−19.3°C). Blended solid deicers with calcium chloride greatly improved the ice melting capacity, especially at lower temperatures. For example, as shown in figure 11, blending 1 g of calcium chloride to 2.3 g of sodium chloride (Sample D-2) increased the melting capacity of the deicer at 1 hour by 45 percent at 26.5°F (−3.1°C), whereas the melting capacity was almost tripled at 8.4°F (−8.1°F) compared to Sample D-1. The improved melting capacity resulted not only from the additional electrolyte applied but also from the heat released by calcium chloride when

it contacted the water. Further increase in the calcium chloride content continued to improve the melting capacity, although at a lower rate. However this will raise the cost of material and be more corrosive to the infrastructure.

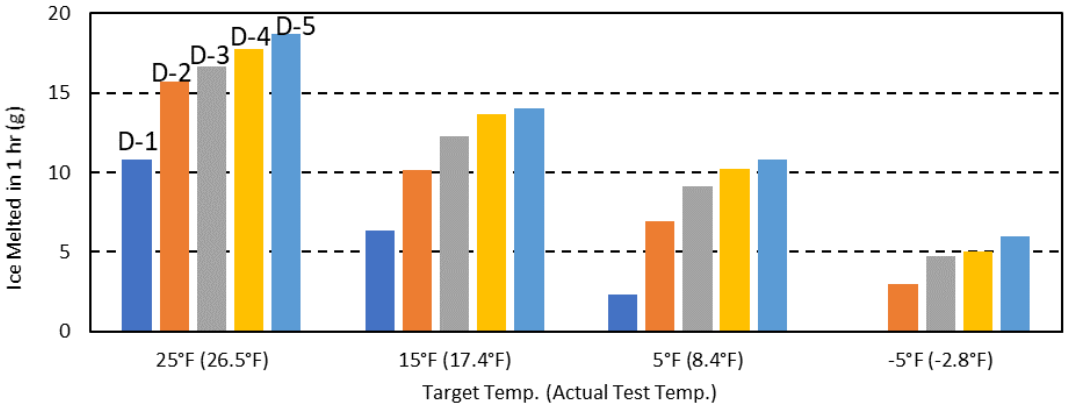

Figure 11. Graph. Ice melting capacity in 1 hour.

SNOW MELTING TEST

The snow melting test was performed to compare the effectiveness of the different brine mixes in melting snow; it should not be used to accurately quantify the effectiveness of the different brine mix. This test was conducted at two different temperatures, namely 21°F and 3°F (−6°C and −16°C).

Snow Melting Test Device and Procedure

For the snow melting test, concrete samples were soaked in the brine solutions for at least 24 hours. The cylinders were then removed from the brine solution and excess brine was left to air dry prior to testing. Rigid transparent plastic sheets were cut to size and wrapped around the concrete cylinders as shown in figure 12.

Figure 12. Photo. Snow melting test setup with plastic sheets wrapped around cylinders (after 1 hour).

The plastic sheets extend 2 inches above the height of the concrete cylinders. Shaved ice was used to simulate snow and was gently placed on top of the concrete cylinders. To produce initial uniform depths, a straightedge was used to remove excess shaved ice that extended beyond the plastic sheeting. The cylinders with the shaved ice were then placed in the freezer for 1 hour. Measurements were taken every hour for 3 consecutive hours to determine the remaining snow depths. The accumulated snow melting depths can be calculated by subtracting the initial 2 inches of snow depth from the leftover depths at the different time intervals. At least six measurements around the cylinder were taken, and the average snow depth was obtained using these six measurements. This test was intended to mimic field conditions where brine was applied prior to snow events.

Snow Melting Test Result

The results of the snow melting test are shown in table 5 and table 6, respectively.

Table 5. Snow melting test for different brine solutions at 21°F.

T=21°F	Accumulated Snow Melt Depth, Inches				
Brine Solution	**0 hr**	**1 hr**	**2 hr**	**3 hr**	**Rank**
B-0 (23% NaCl)	0	0.68	0.89	0.94	1
B-5 (23% NaCl + 5% $CaCl_2$)	0	0.64	0.79	0.77	5
B-10 (23% NaCl + 10% $CaCl_2$)	0	0.52	0.65	0.73	6
B-15 (23% NaCl + 15% $CaCl_2$)	0	0.7	0.9	0.92	2
B-20 (23% NaCl + 20% $CaCl_2$)	0	0.59	0.84	0.82	4
B-25 (23% NaCl + 25% $CaCl_2$)	0	0.67	0.87	0.86	3

Table 6. Snow melting test for different brine solutions at 3°F.

T=3°F	Accumulated Snow Melt Depth, Inches				
Brine Solution	**0 hr**	**1 hr**	**2 hr**	**3 hr**	**Rank**
B-0 (23% NaCl)	0	1.02	1.25	1.25	2
B-5 (23% NaCl + 5% $CaCl_2$)	0	0.96	0.97	1.04	4
B-10 (23% NaCl + 10% $CaCl_2$)	0	1.22	1.31	1.32	1
B-15 (23% NaCl + 15% $CaCl_2$)	0	0.93	1.04	1.09	3
B-20 (23% NaCl + 20% $CaCl_2$)	0	0.86	0.86	0.99	5
B-25 (23% NaCl + 25% $CaCl_2$)	0	0.95	0.99	0.99	5

Since the samples were soaked in brine prior to applying the shaved ice on top, the expected result was melting of the shaved ice over time and, thus, a decrease in its overall depth. At a temperature of 21°F(−6°C), the snow melting table shows that the melting capabilities of the B-0 and B-15 brine mixes are better than others. At a temperature of 3°F(−16°C), the B-10 brine solution outperformed the other brine mixes at every time interval; however, the melting performance of the B-0 brine was comparable to that of the B-10 mix. It should be noted that at both temperatures, the snow melting results for the B-0 brine were consistently ranked among the top, and it is more economical to produce. The overall general trend for tests at both temperatures shows that the most significant melting occurred

during the first hour of the test. After the second hour, the accumulated melted snow depths did not change significantly, indicating that the efficiency of all brine mixes to melt snow decreased after the second hour.

Combining results from both the ice and snow melting test, the data support the fact that the brine mix effectiveness is temperature dependent. For 21°F(−6°C), the use of B-0 (0% $CaCl_2$) will be sufficient; however, at 3°F(−16°C) the benefit of having calcium chloride in the mix becomes more apparent. This finding can be used as a strategy for choosing the type of brine, given the expected temperature during a wintery event (i.e., polar vortex, cold front, warm front, etc.).

RETENTION RATE OF BRINES ON PAVEMENT SURFACE

The retention rate of a brine sample is defined as the percentage of brine that adheres to the pavement surface after the initial application. The retention rate is mainly affected by the type and wet condition of pavements and the type of brines applied.

Retention Test Device and Procedure

A retention test device is shown in figure 13. To obtain the retention ability of pavements, both Portland cement concrete (PCC) and asphalt mixture slabs were made. Two gradations of asphalt mixtures (OGFC-12.5 and Superpave-12.5) were selected for the asphalt mixture slabs (figure 14). Portland cement concrete with a normal maximum aggregate size of 3/4-inch was used for making the PCC slab (figure 15).

Figure 13. Photo. Retention test device.

Figure 14. Photos. OGFC-12.5 (left) and Superpave-12.5 (right) pavement slabs.

Figure 15. Photo. Portland cement concrete slabs.

Retention Rate Result

Data of the solution retention were recorded under dry and submerged conditions and sorted based on the pavement slab type with different slopes. Table 7 summarizes the weight of the three different dry slabs when subject to 20.0 mL of deicer solution. The amount of retention is calculated by subtracting the initial weight of the slab from the final weight of the same slab. The percentage of retention is then the percentage of brine retained on the surface of the slab. Each condition was tested three times and the average percentage of retention was calculated.

The retention ability of the pavement surface is affected by the type of pavement surface, the slope of the pavement, and the condition of wetness. Steep, smooth, and wetted surfaces tend to have lower retention compared to coarse surfaces, and vice versa.

Table 7. Result of retention on dry pavement slabs.

	Slab Types	Initial Weight (g)	Weight after Salt (g)	Retention (g)	Percentage of Retention (%)
Asphalt	Superpave, no slope	9076	9095	19	95
			9094	18	90
			9094	18	90
	Retention average			*18.3*	*91.7*
	Superpave, 10% slope	9076	9084	8	40
			9087	11	55
			9089	13	65
	Retention average			*10.7*	*53.0*
	OGFC, no slope	8930	8950	20	100
			8948	18	90
			8950	20	100
	Retention average			*19.3*	*96.7*
	OGFC, 10% slope	8930	8947	17	85
			8949	19	95
			8948	18	90
	Retention average			*18*	*90*
Concrete	Concrete, no slope	8800	8815	15	75
			8816	16	80
			8815	15	75
	Retention average			*15.3*	*76.7*
	Concrete, 10% slope	8800	8810	10	50
			8809	9	45
			8811	11	55
	Retention average			*10*	*50*

The OGFC pavement had a greater retention amount than the Superpave and concrete pavements. The brine applied tends to quickly infiltrate through the pavement. For 20.0 mL of brine applied, 19.3 mL was retained by the OGFC and 18.3 mL was retained by the Superpave. The volume retained by the concrete was 15.3 mL, which is one-third of the volume applied.

The retention decreased when a 10 percent slope was applied. Slopes increased the volume of brine running out of the surface of the slab. For the Superpave slab, the difference between the retention before and after the application of slope was 7.7 mL, so the Superpave slab lost almost half of its weight due to the 10 percent inclination applied. The amount of brine lost by the OGFC slab was 1.3 mL, which is less than the Superpave pavement lost. The Portland cement concrete lost 5.3 mL of brine.

The retention decreased when the slabs were submerged in water. In fact, the pores were filled with water until saturation, which reduces the amount of salt infiltrated. Each pavement type had a different retention ability when saturated with water. For 20.0 mL of brine applied, 19.1 mL was retained by the OGFC, 12.7 mL by the Superpave, and 11.3 mL by the Portland cement.

SUMMARY

1. The 23% NaCl brine prepared with the GDOT rock salt had a measured freezing point of 3.2°F (−16.0°C).
2. An increase in the dose of calcium chloride in the brines lowered their freezing points. The freezing point of the brine decreased when additional calcium chloride was added into the 23% NaCl brine. The measured freezing point of the blended brine ranged from 2.2°F (−16.6°C) with 5% $CaCl_2$ to 14.8°F (−26.0°C) with 25% $CaCl_2$.
3. When the dose of the GDOT and the pure calcium chloride samples in the brine increased, the time taken to reach its freezing point also increased. The freezing

point of the brines decreased as the dose of sodium chloride in the brines increased. This finding was true for both pure salt and the GDOT salt.

4. The freezing points calculated from the theoretic equation were larger than those of the measured freezing points, depending on the dose of calcium chloride. The maximum difference between the calculated and the measured could be about 17 percent.
5. The penetration of brine to the ice depended on the dose of calcium chloride and the temperature of the ice. The brine of 23% NaCl + 20% $CaCl_2$ had the highest penetration capability for a temperature of 25°F (−4°C). The penetration capability was decreased as the temperature of ice was lowered. There was not penetration until the dose of calcium chloride increased to 23% NaCl + 20% $CaCl_2$ for a temperature of ice of 15°F (-9°C). There was no penetration by all the brines for a temperature of ice of 5°F (−15°C).
6. Sodium chloride had very limited ice melting capacity at 8.4°F (−13.1°C) and almost zero ice melting capacity at −2.8°F (−19.3°C). Blending solid deicers with calcium chloride greatly improved the ice melting capacity, especially at lower temperatures. The improved melting capacity resulted not only from the additional electrolyte applied but also from the heat released by calcium chloride when it contacted water. Further increase in the calcium chloride content continued to improve the melting capacity, although at a lower rate.
7. Combining results from both the ice and snow melting tests, the brine mix effectiveness was temperature dependent. For 21°F(−6°C), the use of the control

(0% $CaCl_2$) was sufficient; however, at 3°F(−16°C) the benefit of having calcium chloride in the mix became more apparent.

8. The surface of the slab affected its retention ability. Smooth surfaces like concrete and Superpave asphalt retained less brine compared to coarse surfaces like OGFC pavement. When the same amount of brine was applied under the same conditions for all the slabs, OGFC had 97 percent retention, Superpave had 92 percent, and Portland cement concrete had 77 percent.
9. When subject to a slope of 10 percent, the retention of all the slabs decreased. In addition, the amount of brine applied to the surface of the slab determined its retention ability. A smaller amount of brine increased retention ability. Further, the dry condition of the slab bettered its ability to retain a brine solution.

CHAPTER 3. THE EFFECTS OF BRINES ON THE PERFORMANCE OF ASPHALT BINDERS

INTRODUCTION

Asphalt concretes are mixtures of aggregates and asphalt binders. If brines are to impact the properties of an asphalt concrete mixture, the effect may be on the asphalt binder, the aggregate, or both. This chapter examines how the brine affects the asphalt binders through laboratory tests. The scope of this study was limited to the effect of blended sodium and calcium chlorides at five different percentages on four asphalt binders, including three modified asphalt binders and one unmodified binder. Asphalt binder samples were prepared and soaked in brines for durations of 7 days and 28 days. Dynamic shear rheometer (DSR) and bending beam rheometer (BBR) were used to test the brine-soaked asphalt binders in different states: without aging, RTFO residuals, and PAV residuals. Control samples without brine-soaking were also tested for comparison purposes. In addition, the microscopic properties of asphalt binders were tested with the atomic force microscopy (AFM).

MATERIALS AND TEST PROCEDURES

Materials

Four asphalt binders (three different modified and one unmodified) were sampled from plants in Georgia. The modified asphalt binders tested are ground tire rubber hybrid (GTRH) modified, polymer-modified asphalt (PMA) modified, and styrene–butadiene–

styrene (SBS) modified. All three modified binders have a performance grade (PG) of 76-22. The unmodified binder (UM) tested has a PG of 64-22.

Five brine samples (denoted as “D1” to “D5”) were prepared with 23% NaCl and varying percentages of calcium chlorides. The blend ratios of the five brines are shown in table 8.

Table 8. Combination of the dose of different salts.

Salts	D1	D2	D3	D4	D5
NaCl (%)	23	23	23	23	23
$CaCl_2$(%)	0	10	15	20	25

The salt materials used to prepare the brine samples are described in Chapter 2. A notable observation during the brine preparation is that the calcium chloride would settle to the bottom of the jars. Figure 16-A shows the solutions near fully dissolved, and figure 16-B shows when the calcium chloride and remaining sodium chloride had settled.

(A) Brines nearly fully dissolved (B) Brines after settlement

Figure 16. Photo. Solutions D2, D3, D4, and D5.

Sample Preparation

Asphalt binder beams for the BBR test were made as shown in figure 17. A total of 360 asphalt binder beams of the four different asphalt binders were made (see figure 18). The asphalt beams were soaked in the brines in glass jars with airtight lids for the durations of 7 and 28 days before testing to represent a short- and long-term contact of brines on the asphalt pavement in real-world applications. Also, while the beams were soaking, they were kept in a refrigerator at a temperature between 30°F and 35°F. The airtight lids were used so that there was no escape of water. Nine asphalt beams were placed in each jar and each type of concentration of brines. To keep the salts dissolved as uniformly as possible, the jars were shaken every 4 hours during the daytime.

Figure 17. Photo. Pouring asphalt binder into molds.

Figure 18. Photo. Asphalt binder beams soaking in jars with different brines.

Test Procedures

To investigate the effect of the brines on the asphalt binders, the rheological properties at high and intermediate temperatures were tested using a DSR (ASTM D7552[13]) on samples of the soaked asphalt binders without aging, RTFO (ASTM D2872[14]) residual, and PAV (ASTM D6521[15]) residual, as well. The creep properties at low temperatures were tested using BBR (ASTM D6648[16]) for the PAV residuals of soaked asphalt binders. Tests were performed on control samples that were not soaked for comparison purposes. The equipment used for the tests is shown in figure 19.

(a) Dynamic Shear Rheometer

(b) Bending Beam Rheometer

(c) Rolling Thin Film Oven

(d) Pressure Aging Vessel

Figure 19. Photos. Apparatus used for this project: (a) DSR, (b) BBR, (c) RTFO, (d) PAV.

For this study, the NanoSurf FlexAFM system (figure 20) was used to characterize of the mechanical properties (Young's modulus and adhesion) of the asphalt binder. The cantilever (probe) used for these experiments was SHOCON of 225 µm long, 46 µm wide,

1.0 µm thick, and with a natural frequency of 8-37 kHz. The Nanosurf Easyscan 2 version 3.8.8.7 software was used for capturing the topographical images which were processed to obtain the spectroscopic data of each asphalt binder tested. Deflection sensitivity calibration and spring constant calibration were performed to maximize the frequency of data obtained. The image size was selected as 30 µm × 30 µm with 512 pixels of a display.

Figure 20. Photo. Atomic force microscope (AFM).

RESULTS AND DISCUSSIONS

Rheological Properties of Asphalt Binders Soaked for 7 and 28 days (without aging)

Overall, the responses of the modified binders to the brines were different from those of the unmodified binder. The G*/sin(δ) of the modified binders increased and that of the unmodified binder decreased by soaking in the 23% NaCl brine. In addition, a general trend

was that the G*/sin(δ) of the modified asphalt binders increased as the dose of calcium chloride increased, but mixed results were observed for the unmodified binder (see figure 21). Further, slight increases in a high dose of brines of calcium chloride were observed. As compared to the controls, GTRH modified binders showed the least increase in the G*/sin(δ) as the dose of brines changed, followed by the SBS modified binders, although all these increases were not high.

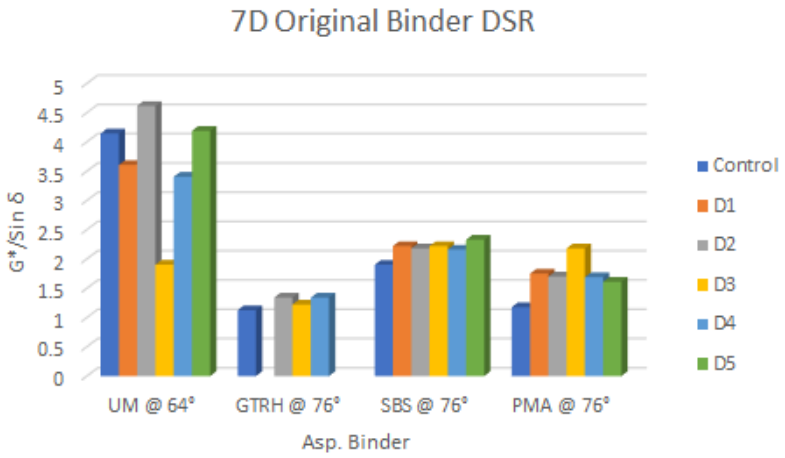

Figure 21. Graph. The G*/sin(δ) of the asphalt binders soaked for 7 days (without aging).

Analysis of variance (ANOVA) was conducted to understand the differences of the G*/sin(δ) caused by the type of asphalt binder and the dose of calcium chloride. The results are listed in table 9. The difference between the G*/sin(δ) caused by the type of binder seemed to be significant, and that by dose of calcium chloride was not significant. A detailed comparison between the binders and between the dose of calcium chloride was conducted and the results are listed in table 10 and table 11. The most significant difference

was found between the unmodified binder and the PMA modified binder with a p-value of 0.024.

Table 9. ANOVA for 7-day pre-RTFO G*/sin(δ).

	DF	Sum Sq	Mean Sq	F-Value	p-Value
Binder	3	3.268	1.089	3.749	0.034*
Brine	5	0.856	0.171	0.590	0.708
Residual	15	4.358	0.290	--	--

*Significant (p-value<0.05)

Table 10. Tukey multiple comparison between binders, 7-day pre-RTFO G*/sin(δ).

	Difference	Lower Bound	Upper Bound	p-Value
PMA–GTRH	0.403	−0.494	1.300	0.580
SBS–GTRH	0.094	−0.803	0.991	0.990
UM–GTRH*	−0.614	−1.511	0.283	0.241
SBS–PMA	−0.308	−1.205	0.589	0.757
UM–PMA	−1.017	−1.914	−0.120	0.024
UM–SBS	−0.708	−1.605	0.189	0.148

* UM = Unmodified

Table 11. Tukey multiple comparison between brines, 7-day pre-RTFO G*/sin(δ).

	Difference	Lower Bound	Upper Bound	p-Value
D2–D1	0.246	−0.993	1.484	0.985
D3–D1	−0.329	−1.568	0.909	0.950
D4–D1	−0.067	−1.305	1.172	1.000
D5–D1	0.163	−1.076	1.401	0.998

The effect of brines on the asphalt binders soaked for 28 days can be observed in figure 22. After soaking, the G*/sin(δ) of the GTRH modified binder increased, while that of the SBS and PMA modified binders decreased, and that of the unmodified binder increased. Further, the G*/sin(δ) of most of the binders increased as the dose of calcium chloride increased.

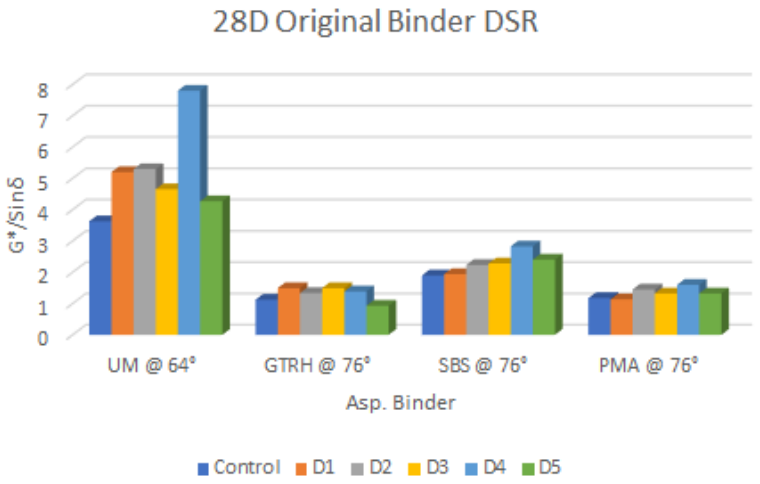

Figure 22. Graph. The G*/sin(δ) of the asphalt binders soaked for 28 days (without aging).

Statistical analyses were also conducted by ANOVA to understand the differences of the G*/sin(δ) caused by the type of asphalt binder and the dose of calcium chloride. The results are listed in table 12. Similar to those soaked for 7 days, the p-value for type of asphalt binder was less than 0.05, whereas that for the dose of calcium chloride was larger than 0.05. The difference between the G*/sin(δ) caused by the type of binder was significant, and that by the dose of calcium chloride was not significant. A detailed comparison between the binders and between the dose of calcium chloride was conducted and the results are listed in table 13 and table 14. The multiple analysis result also indicates that the GTRH sample behaved differently than the other three samples.

The rheological property, G*/sin(δ), of original binders after soaking was observed to increase slightly regardless of the duration of soaking, indicating the rutting resistance of the tested binders is, therefore, not negatively affected by soaking.

Table 12. ANOVA for 28-day pre-RTFO G*/sin(δ).

	DF	Sum Sq	Mean Sq	F-Value	p-Value
Binder	3	9.887	3.296	7.206	0.003*
Brine	5	4.556	0.911	1.992	0.138
Residual	15	6.860	0.457	--	--

*Significant (p-value<0.05)

Table 13. Tukey multiple comparison between binders, 28-day pre-RTFO G*/sin(δ).

	Difference	Lower Bound	Upper Bound	p-Value
PMA–GTRH	−1.300	−2.425	−0.175	0.021
SBS–GTRH	−1.558	−2.684	−0.433	0.006
UM–GTRH	−1.533	−2.659	−0.408	0.007
SBS–PMA	−0.258	−1.384	0.867	0.910
UM–PMA	−0.233	−1.359	0.892	0.931
UM–SBS	0.025	−1.100	1.150	1.000

Table 14. Tukey multiple comparison between brines, 28-day pre-RTFO G*/sin(δ).

	Difference	Lower Bound	Upper Bound	p-Value
D2–D1	0.125	−1.429	1.679	1.000
D3–D1	−0.025	−1.579	1.529	1.000
D4–D1	0.938	−0.616	2.491	0.407
D5–D1	−0.200	−1.754	1.354	0.998

Rheological Properties of Asphalt Binders Soaked for 7 and 28 days (RTFO residuals)

The values of the G*/sin(δ) of the modified binders were somewhat decreased and that of the unmodified binder increased after being soaked in the brine of 23% NaCl (see figure 23). In addition, a general trend that the G*/sin(δ) of both the modified and unmodified asphalt binders increased with an increased dose of calcium chloride was observed, except for the PMA modified binder which showed little change in G*/sin(δ).

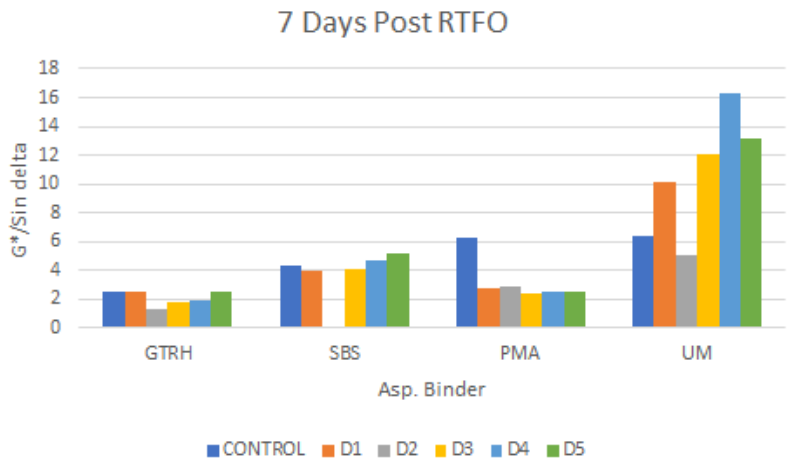

Figure 23. Graph. G*/sin(δ) of asphalt binders after 7 days soaking (RTFO residual).

Statistical analyses were conducted by ANOVA to understand the differences of the G*/sin(δ) caused by the type of asphalt binder and the dose of calcium chloride. The results are listed in table 15. Only the p-values for type of binder were less than 0.05, indicating that there is significant difference between the G*/sin(δ) caused by the type of binder, but not by the dose of calcium chloride. Multiple comparison (table 16 and table 17) confirmed

that the UM binder showed significantly more increase in G*/sin(δ) with increased dose of calcium chloride compared to the other three binders.

Table 15. ANOVA for 7-day post-RTFO G*/ sin(δ).

	DF	Sum Sq	Mean Sq	F-Value	p-Value
Binder	3	170.27	56.76	9.957	<0.001*
Brine	5	22.34	4.47	0.784	0.577
Residual	15	85.51	5.70	--	--

*Significant (p-value<0.05)

Table 16. Tukey multiple comparison between binders, 7-day post-RTFO G*/sin(δ).

	Difference	Lower Bound	Upper Bound	p-Value
PMA–GTRH	0.403	−0.494	1.300	0.580
SBS–GTRH	0.894	−0.003	1.791	0.051
UM–GTRH	2.386	1.489	3.283	<0.001*
SBS–PMA	0.492	−0.405	1.389	0.418
UM–PMA	1.983	1.086	2.880	<0.001*
UM–SBS	1.492	0.595	2.389	0.001*

*Significant (p-value<0.05)

Table 17. Tukey multiple comparison between brines, 7-day post-RTFO G*/sin(δ).

	Difference	Lower Bound	Upper Bound	p-Value
D2–D1	−1.500	−6.985	3.985	0.944
D3–D1	0.325	−5.160	5.810	1.000
D4–D1	1.600	−3.885	7.085	0.927
D5–D1	1.025	−4.460	6.510	0.989

The values of the G*/sin(δ) of all RTFO residuals of the asphalt binders after soaking for 28 days and the controls are listed in figure 24. Again, the G*/sin(δ) of PMA and GTRH modified binders soaked in sodium chloride decreased, while those of the soaked SBS modified and unmodified binders increased. Further, as the dose of calcium chloride increased, the G*/sin(δ) of the SBS modified and unmodified binders increased, whereas those of the GTRH and PMA modified binders decreased.

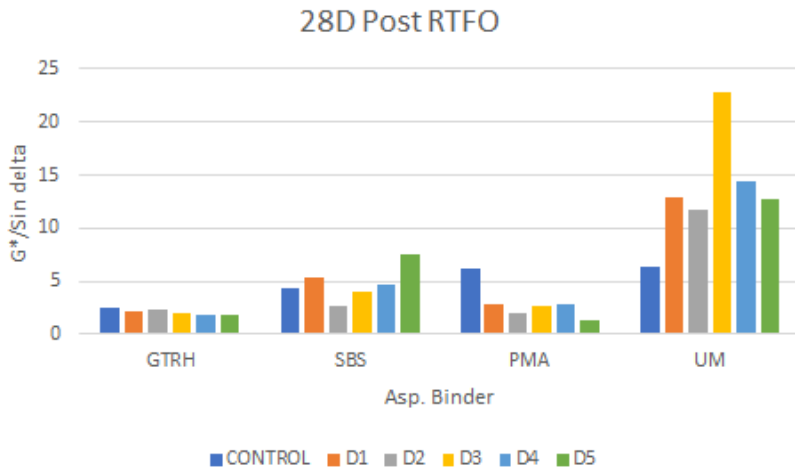

Figure 24. Graph. G*/sin(δ) of asphalt binders after 28 days soaking (RTFO residuals).

Statistical analyses were conducted by ANOVA to understand the differences of the G*/sin(δ) caused by the type of asphalt binder and the dose of calcium chloride. The results are listed in table 18. The p-value for type of binder was less than 0.05, whereas that for dose of calcium chloride was larger than 0.05, indicating that there is a significant difference between the G*/sin(δ) caused by the type of binder, but not by the dose of calcium chloride. Multiple comparison (table 19 and table 20) confirmed that the UM

binder showed significantly more increase in G*/sin(δ) with increased dose of calcium chloride compared to the other three binders.

Table 18. ANOVA for 28-day post-RTFO G*/sin(δ).

	DF	Sum Sq	Mean Sq	F-Value	p-Value
Binder	3	371.8	123.93	12.704	<0.001*
Brine	5	23.7	4.75	0.487	0.781
Residual	15	146.3	9.75	--	--

*Significant (p-value<0.05)

Table 19. Tukey multiple comparison between binders, 28-day post-RTFO G*/sin(δ).

	Difference	Lower Bound	Upper Bound	p-Value
PMA–GTRH	−3.100	−8.297	2.097	0.348
SBS–GTRH	0.683	−4.514	5.880	0.981
UM–GTRH	7.667	2.470	12.864	0.003*
SBS–PMA	3.783	−1.414	8.980	0.198
UM–PMA	10.767	5.570	15.964	<0.001*
UM–SBS	6.983	1.786	12.180	0.007*

*Significant (p-value<0.05)

Table 20. Tukey multiple comparison between brines, 28-day post-RTFO G*/sin(δ).

	Difference	Lower Bound	Upper Bound	p-Value
D2–D1	−0.950	−8.125	6.225	0.998
D3–D1	2.000	−5.175	9.175	0.939
D4–D1	0.175	−7.000	7.350	1.000
D5–D1	0.150	−7.025	7.325	1.000

Rheological Properties of Asphalt Binder Soaked 7 and 28 days (PAV residuals)

The values of the G*sin(δ) of D1s (23% NaCl + 0% $CaCl_2$) for 7 days soaking, as compared with those of the controls, were increased for the GTRH and SBS modified binders, and decreased for the PMA modified binder (see figure 25). The G*sin(δ) of the unmodified binder when soaked increased. The effect of the soaking in brines on the G*sin(δ) was mixed, depending on the type of binder.

Further, a vague trend was observed that a higher concentration of calcium chloride caused a slight change in the G*sin(δ) of the modified asphalt binders, but an obvious increase for unmodified binders. The G*sin(δ) of the PMA modified binders responded to the dose of calcium chloride.

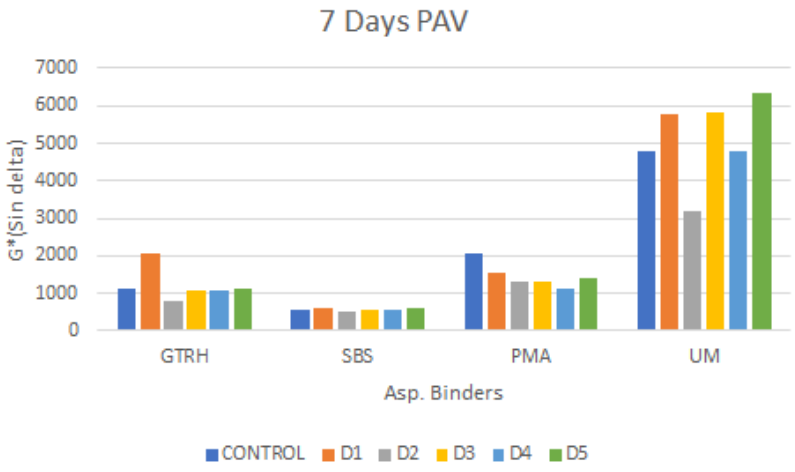

Figure 25. Graph. The G*sin(δ) of asphalt binders soaked 7 days (PAV residuals).

In conclusion, the effect of sodium chloride brine on the fatigue resistance of the soaked modified binders was mixed, either degraded or enhanced, depending on the type of binder discussed. The dose of calcium chloride did not have much effect on the fatigue resistance

of the modified binders regardless of the type, while the unmodified binder indicated obvious degradation after soaking.

ANOVA (table 21) and multiple comparison (table 22 and table 23) showed that neither binder type nor brine type had a significant difference in the trend.

Table 21. ANOVA for 7-day PAV G*sin(δ).

	DF	Sum Sq	Mean Sq	F-Value	p-Value
Binder	3	2749479	916493	2.646	0.087
Brine	5	2776771	555354	1.603	0.219
Residual	15	5196146	346410	--	--

Table 22. Tukey multiple comparison between binders, 7-day PAV G*/sin(δ).

	Difference	Lower Bound	Upper Bound	p-Value
PMA–GTRH	−658.333	−1637.712	321.046	0.255
SBS–GTRH	−50.000	−1029.379	929.379	0.999
UM–GTRH	266.667	−712.712	1246.046	0.860
SBS–PMA	608.333	−371.046	1587.712	0.316
UM–PMA	925.000	−54.379	1904.379	0.067
UM–SBS	316.667	−662.712	1296.046	0.788

Table 23. Tukey multiple comparison between brines, 7-day PAV G*/sin(δ).

	Difference	Lower Bound	Upper Bound	p-Value
D2–D1	−1050.000	−2402.152	302.152	0.178
D3–D1	−300.000	−1652.152	1052.152	0.976
D4–D1	−612.500	−1964.652	739.652	0.686
D5–D1	−162.500	−1514.652	1189.652	0.999

The effect of the brines on the G*sin(δ) of the asphalt binder's PAV residuals for 28 days soaking is shown in figure 26. All the modified asphalt binders showed an increase in the G*sin(δ) of the modified binders, whereas the unmodified binder had a decrease in the G*sin(δ). The dose of calcium chloride, in general, decreased the G*sin(δ) for all the modified asphalt binders and increased the G*sin(δ) of the unmodified asphalt binder. The GTRH and SBS modified binders responded to the dose of calcium chloride to a much larger degree than the PMA modified binder.

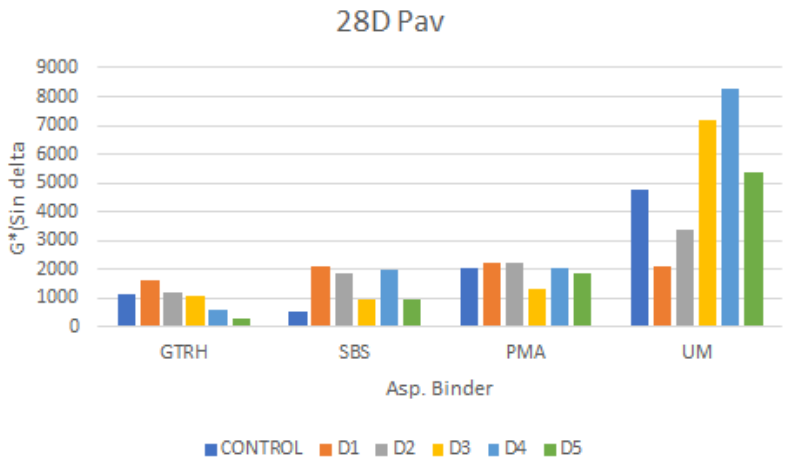

Figure 26. Graph. The G*sin(δ) of asphalt binders soaked 28 days (PAV residuals).

ANOVA was conducted to understand the differences of the G*sin(δ) caused by the type of asphalt binder and the dose of calcium chloride. The results are listed in table 21 for soaking 7 days and table 24 for soaking 28 days. The p-values for type of binder and dose of calcium chloride were larger than 0.05, regardless of the duration of soaking. Detailed comparisons between the binders and between the dose of calcium chloride were conducted and the results are listed in and table 23 for 7 days soaking and table 25 and table 26 for 28 days soaking. Again, there were no significant differences between the values of the G*sin(δ) caused by either the type of binder or the dose of calcium chloride.

The G*sin(δ) is used as a parameter to evaluate the fatigue resistance of asphalt binders. The lower the value of the parameter, the better the rutting resistance. The G*sin(δ) of the asphalt binders was slightly increased in general after being soaked in the brine of 23% NaCl, and then decreased with the continued addition of calcium chloride. The differences of increase and decrease in G*sin(δ) were, however, insignificant with regard to the type of binder and the dose of calcium chloride.

Table 24. ANOVA for 28-day PAV G*sin(δ).

	DF	Sum Sq	Mean Sq	F-Value	p-Value
Binder	3	5005833	1668611	0.948	0.442
Brine	5	4468750	893750	0.508	0.766
Residual	15	26405417	1760361	--	--

Table 25. Tukey multiple comparison between binders, 28-day PAV G*sin(δ).

	Difference	Lower Bound	Upper Bound	p-Value
PMA–GTRH	58.564	−2149.748	2266.200	1.000
SBS–GTRH	1142.322	−1066.556	3349.528	0.467
UM–GTRH	500.236	−1707.102	2708.641	0.913
SBS–PMA	1083.865	−1124.033	3291.902	0.510
UM–PMA	442.854	−1766.564	2649.012	0.938
UM–SBS	−642.231	−2849.901	1566.203	0.836

Table 26. Tukey multiple comparison between brines, 28-day PAV G*sin(δ).

	Difference	Lower Bound	Upper Bound	p-Value
D2–D1	162.774	−2886.231	3211.300	1.000
D3–D1	650.502	−2398.205	3698.033	0.980
D4–D1	1238.705	−1811.744	4286.897	0.771
D5–D1	138.056	−2911.202	3186.414	1.000

Creep Properties of Asphalt Binders Soaked for 7 and 28 Days (PAV Residuals)

The stiffnesses of the PAV residuals for the asphalt binders after 7 and 28 days soaking are presented in figure 27 and figure 28, respectively. A general trend was that the stiffnesses of D1 samples (soaked in 23% NaCl brine) decreased as compared with the controls for all the asphalt binders soaked for 7 and 28 days. Further, the stiffnesses of most of the binders decreased slightly as the dose of calcium chloride increased, except for the GTRH binder. ANOVA (table 27 and table 30) did not show a significant effect from either the 7-day or 28-day brine soaking. Multiple comparison shows that the GTRH behaved differently from

the other three binders in 7 days of soaking (table 28 and table 29), but the difference became insignificant after 28 days of soaking (table 31 and table 32).

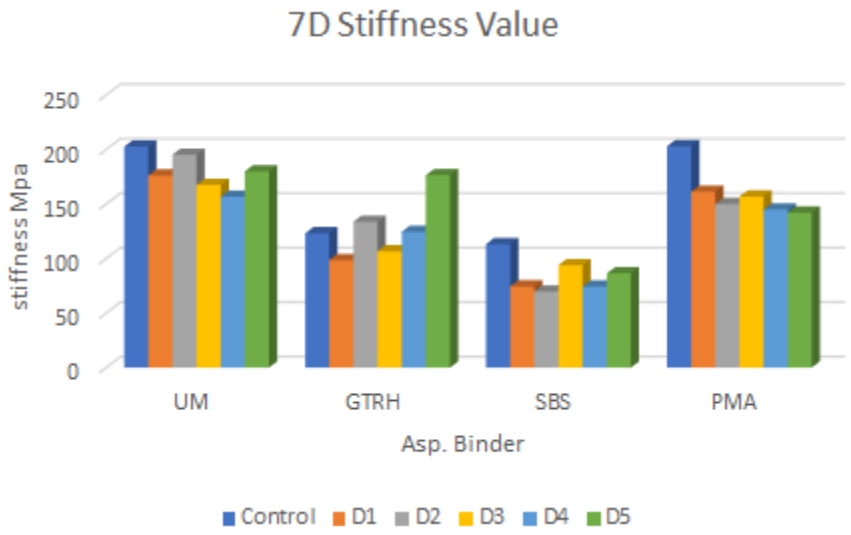

Figure 27. Graph. Stiffness of asphalt binder after 7 days soaking (PAV residuals).

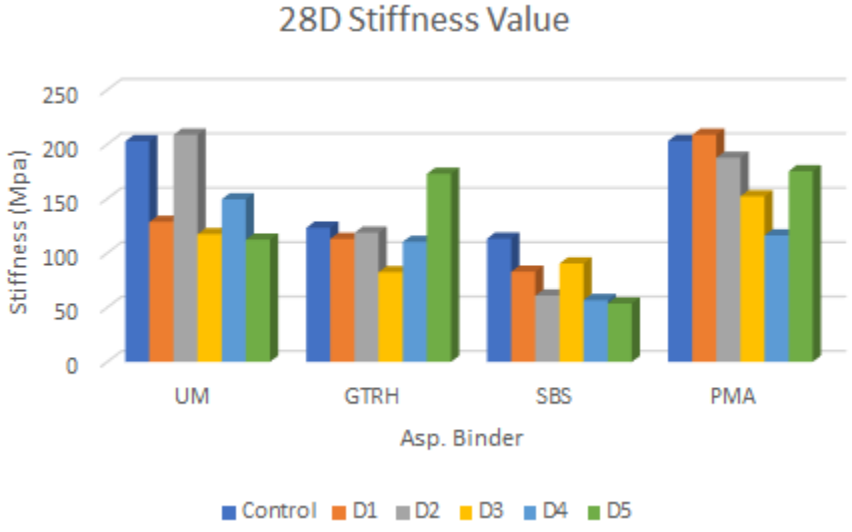

Figure 28. Graph. Stiffness of asphalt binders after 28 days soaking (PAV residuals).

Table 27. ANOVA for 7-day PAV stiffness.

	DF	Sum Sq	Mean Sq	F-Value	p-Value
Binder	3	7353	2451.2	6.532	0.004*
Brine	5	4418	883.5	2.355	0.091
Residual	15	5628	375.2	--	--

*Significant ($p<0.05$)

Table 28. Tukey multiple comparison between binders, 7-day PAV stiffness.

	Difference	Lower Bound	Upper Bound	p-Value
PMA–GTRH	−47.500	−79.732	−15.268	0.003*
SBS–GTRH	−35.833	−68.066	−3.601	0.027*
UM–GTRH	−27.500	−59.732	4.732	0.108
SBS–PMA	11.667	−20.566	43.899	0.728
UM–PMA	20.000	−12.232	52.232	0.317
UM–SBS	8.333	−23.899	40.566	0.877

*Significant difference ($p<0.05$)

Table 29. Tukey multiple comparison between brines, 7-day PAV stiffness.

	Difference	Lower Bound	Upper Bound	p-Value
D2–D1	11.250	−33.251	55.751	0.959
D3–D1	2.500	−42.001	47.001	1.000
D4–D1	−1.250	−45.751	43.251	1.000
D5–D1	18.750	−25.751	63.251	0.744

Table 30. ANOVA for 28-day PAV stiffness.

	DF	Sum Sq	Mean Sq	F-Value	p-Value
Binder	3	6435	2145.2	2.223	0.128
Brine	5	8378	1675.5	1.737	0.187
Residual	15	14472	964.8	--	--

Table 31. Tukey multiple comparison between binders, 28-day PAV stiffness.

	Difference	Lower Bound	Upper Bound	p-Value
PMA–GTRH	−24.333	−76.019	27.352	0.543
SBS–GTRH	−28.667	−80.352	23.019	0.409
UM–GTRH	−45.833	−97.519	5.852	0.091
SBS–PMA	−4.333	−56.019	47.352	0.995
UM–PMA	−21.500	−73.186	30.186	0.637
UM–SBS	−17.167	−68.852	34.519	0.775

Table 32. Tukey multiple comparison between brines, 28-day PAV stiffness.

	Difference	Lower Bound	Upper Bound	p-Value
D2–D1	10.250	−61.109	81.609	0.997
D3–D1	−23.250	−94.609	48.109	0.890
D4–D1	−23.500	−94.859	47.859	0.886
D5–D1	−3.750	−75.109	67.609	1.000

The m-values of PAV residuals for asphalt binders soaked for 7 and 28 days are presented in figure 29 and figure 30, respectively. Overall, the m-values of the soaked asphalt binders were not affected as much as stiffnesses were by brine soaking. The m-values of five out

of the eight asphalt binders increased as compared to those of the control samples. In addition, the m-values did not respond as much to the increase of the dose of calcium chloride.

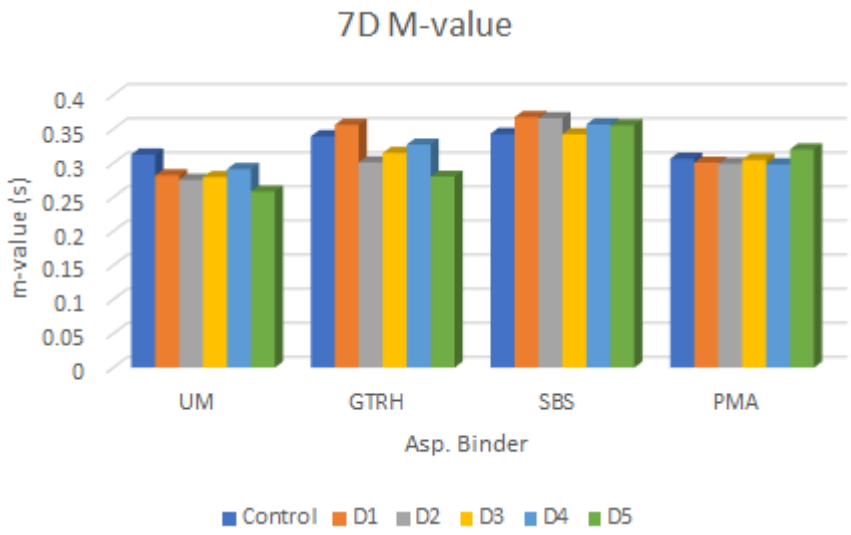

Figure 29. Graph. m-Values of asphalt binders after 7 days soaking (PAV residuals).

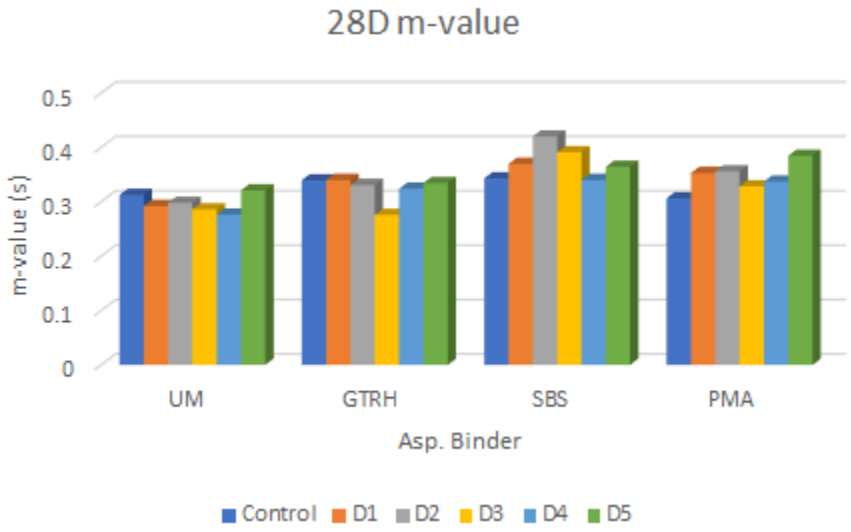

Figure 30. Graph. m-Values of asphalt binders after 28 days soaking (PAV residuals).

Statistical analyses were conducted by ANOVA to understand the differences of the m-values caused by the type of asphalt binder and the dose of calcium chloride. The results are listed in table 33 for soaking 7 days and table 36 for soaking 28 days. The p-value is less than 0.05 for the type of binder for both 7 and 28 days, which indicates significant differences of m-value caused by the type of binder for both 7 and 28 days soaking. Multiple comparisons (see table 34 and table 35 for 7-day, and table 37 and table 38 for 28-day) revealed that the increase of m-value with calcium chloride dosage is more evident in PMA after 7-day soaking (table 34) and in PMA and SBS samples after 28-day soaking (table 37).

Table 33. ANOVA for 7-day PAV m-value.

	DF	Sum Sq	Mean Sq	F-Value	p-Value
Binder	3	0.005353	0.001784	5.977	0.007
Brine	5	0.001843	0.000369	1.234	0.341
Residual	15	0.004478	0.000299		

*Significant ($p<0.05$)

Table 34. Tukey multiple comparison between binders, 7-day PAV m-value.

	Difference	Lower Bound	Upper Bound	p-Value
PMA–GTRH	0.018	−0.011	0.046	0.332
SBS–GTRH	0.030	0.001	0.059	0.039*
UM–GTRH	−0.008	−0.037	0.020	0.837
SBS–PMA	0.013	−0.016	0.041	0.605
UM–PMA	−0.026	−0.055	0.003	0.086
UM–SBS	−0.038	−0.067	-0.010	0.008*

*Significant difference ($p<0.05$)

Table 35. Tukey multiple comparison between brines, 7-day PAV m-value.

	Difference	Lower Bound	Upper Bound	p-Value
D2–D1	−0.020	−0.060	0.020	0.589
D3–D1	−0.016	−0.056	0.023	0.765
D4–D1	−0.009	−0.048	0.031	0.977
D5–D1	−0.023	−0.062	0.017	0.471

Table 36. ANOVA for 28 day PAV m-value.

	DF	Sum Sq	Mean Sq	F-Value	p-Value
Binder	3	0.012511	0.00417	7.553	0.003*
Brine	5	0.004055	0.000811	1.469	0.258
Residual	15	0.008282	0.000552	--	--

*Significant ($p<0.05$)

Table 37. Tukey multiple comparison between binders, 28-day PAV m-value.

	Difference	Lower Bound	Upper Bound	p-Value
PMA–GTRH	0.043	0.003	0.082	0.031*
SBS–GTRH	0.049	0.010	0.088	0.012*
UM–GTRH	0.001	−0.038	0.040	1.000
SBS–PMA	0.007	−0.032	0.046	0.960
UM–PMA	−0.042	−0.081	−0.003	0.035*
UM–SBS	−0.048	−0.087	−0.009	0.013*

*Significant difference ($p<0.05$)

Table 38. Tukey multiple comparison between brines, 28-day PAV m-value.

	Difference	Lower Bound	Upper Bound	p-Value
D2–D1	0.013	−0.041	0.066	0.972
D3–D1	−0.015	−0.069	0.039	0.940
D4–D1	−0.019	−0.073	0.035	0.862
D5–D1	0.015	−0.039	0.069	0.940

The decrease in stiffnesses and increase in m-values of an asphalt binder indicate an improvement in the thermal crack resistance under low temperatures. The soaking of all the asphalt binders in 23% NaCl brine generally caused a decrease in the stiffnesses, and an increase in the m-values indicated some degree of improvement of the low-temperature properties. The effect of the dose of calcium chloride, in general, decreased the stiffnesses and increased slightly the m-values of the asphalt binders, and again improved their low-temperature properties.

Modulus and Adhesion of Asphalt Binders Soaked for 7 Days (without aging)

The Young's modulus (MPa) measured from the asphalt binder samples are presented in figure 31. Higher values of modulus were observed with the control samples. After soaking in the D1 brine, the Young's modulus of the asphalt sample decreased by 20%, 82%, 85% and 81% for UM, GTRH, PMA and SBS binders, respectively. Furthermore, the Young's modulus further decreased with the increase of salt concentration. The results obtained showed that the deicer has a significant impact on the modulus of the asphalt binders, especially for the modified binders.

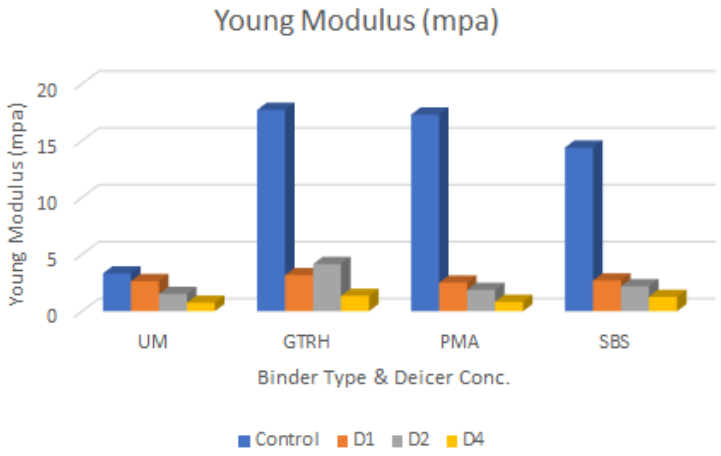

Figure 31. Graph. Young's modulus against concentration of deicer.

The adhesion of an asphalt binder sample in AFM can be done by measuring the adhesive dip in a force curve collected through force spectroscopy. The data processing is very similar to that of the Young's modulus. All operations were done in the contact mode and the force curves obtained from the spectroscopy was processed using the AtomicJ[17] or ANA[18] programs. The Sneddon method of processing was selected. From the results obtained the adhesion force properties were noticeable reduced with the effective

concentration of deicers. The adhesion was measured on different asphalt binders are presented in figure 32. A decrease in adhesion was observed after soaking from all four types of binders tested. In general, the adhesion of the binder forces decreased more when the binder is soaked in a higher concentration brine.

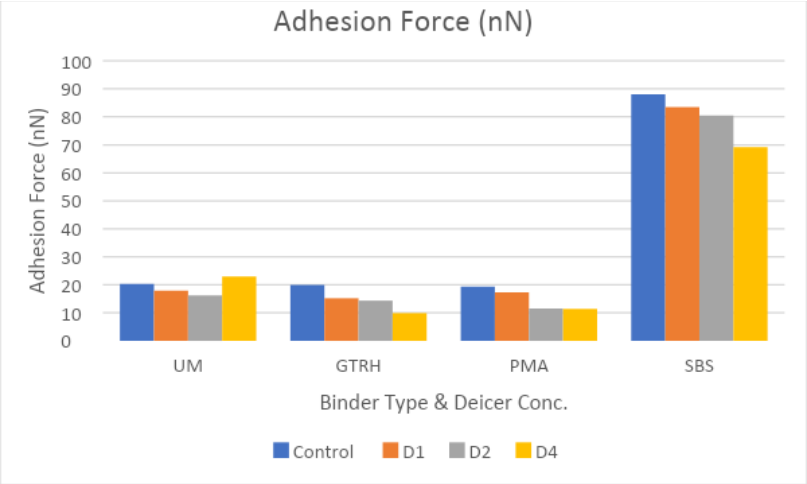

Figure 32. Graph. Adhesion force against the concentration of deicers.

SUMMARY

The effects of brines on the performance properties of asphalt binders were investigated. Four asphalt binders were soaked for 7 and 28 days in the solutions of five various doses of calcium chloride and a fixed dose of sodium chloride. The soaked asphalt binders at three aging statuses, i.e., without aging, RTFO residuals, and PAV residuals, were then tested by DSR and BBR at high, intermediate, and low temperatures. Asphalt binders without soaking were tested as controls. The following conclusions were drawn:

1. The rheological property at high temperatures, G*/sin(δ), of the original binders and RTFO residuals after soaking were observed to increase slightly regardless of

the duration of soaking, indicating the rutting resistance of the tested binders was therefore not negatively affected by soaking. There was a significant difference of G*/sin(δ) caused by the type of binder, i.e., the unmodified binders were more sensitive to soaking in brines.

2. The G*sin(δ) at intermediate temperatures was generally slightly increased after being soaked in the brine of 23% NaCl, and then decreased with the continued addition of calcium chloride. The differences of increase and decrease in G*sin(δ) were, however, insignificant with regard to the type of binder and the dose of calcium chloride.

3. The soaking of all the asphalt binders in 23% NaCl brine caused a general decrease in the stiffnesses, and an increase in the m-values indicated some degree of improvement of the low-temperature properties. The effect of the dose of calcium chloride, in general, decreased the stiffnesses and increased slightly the m-values of the asphalt binders, and again improved their low-temperature properties. Both the creep properties of stiffness and m-value have significant differences caused by the type of binder.

4. Soaking of asphalt binders in solutions of deicers decreased the Young's modulus and adhesion force regardless of the type of asphalt binders. Furthermore, both Young's modulus and adhesion decreased as the dose of deicers in the solution increased.

CHAPTER 4. THE EFFECT OF BRINES ON THE PROPERTIES OF PCC

INTRODUCTION

The brine solution is fundamentally liquid chloride, so its corrosive nature could influence the performance and durability of road infrastructure, just like solid rock salt. As seen in the field, brine can induce cracks or surface spalling in Portland cement concrete, especially during the freeze–thaw (F–T) cycles, often yielding functional and structural degradations. Also, if PCC is exposed to brine for extended periods without any significant winter event, the resistance of PCC to chloride ion penetration may decrease even at high temperatures. This could make steel reinforcements, as well as concrete, more vulnerable to future weathering events. All these hypotheses, however, have not been proven yet and must be investigated in order to implement winter maintenance that minimizes the damages in road infrastructure, such as pavements, bridge decks, and box culverts.

Focusing on the impact of brine solutions—made with the mix of calcium chloride and sodium chloride—on PCC pavement, this chapter presents an experimental study on how PCC's resistance to chloride ions and its impact on performance vary with climatic conditions and brine concentrations. Electric surface resistivity and impact resonance of PCC were selected as two critical performance indicators under two field conditions: long-term erosion at ambient temperatures and rapid F–T cycles. Also, the corrosion potential of epoxy-coated (EC) dowel bars was evaluated with brine-treated concrete samples that were later subjected to a series of F–T cycles followed by a long-term dry erosion in the

air. Finally, the melting capacity of brine solutions was tested with snow and ice samples at selected temperatures.

RESEARCH METHOD

Materials

Table 39 shows the brine solutions proposed by GDOT and tested for their individual impacts on the PCC specimens and dowel bars, and their melting capacity at low temperatures. Following GDOT's practices and recommendations, the research team produced six types of brine solutions by changing the concentration of calcium chloride from 0% to 25% at intervals of 5 percent, while maintaining that of sodium chloride at 23%.

Table 39. Proportions of brine solutions by weight of water.

Designation	Concentration, Weight %	
	NaCl	$CaCl_2$
B-0	23	0
B-5	23	5
B-10	23	10
B-15	23	15
B-20	23	20
B-25	23	25

During production, it was observed that the solubility of calcium chloride was significantly affected by the temperature of water alongside the speed of agitation, especially at concentrations higher than 15% $CaCl_2$. Therefore, solid pellets of both calcium chloride

and sodium chloride were heated in water to completely dissolve all solid particles, as seen in figure 33. For this study, two 5-gallon buckets of brine (brine buckets) per each concentration level were prepared (i.e., 12 brine buckets in total). The GDOT district maintenance office in Lafayette, Georgia, provided all raw materials—the rock salt and calcium chloride pellets—for this study.

(a) Proportioning (left) and mixing in warm water (right)

(b) Brine solution buckets
(two 5-gallon buckets for each concentration)

Figure 33. Photos. Laboratory production of brine solution.

A general-purpose and mildly sulfate-resistant cement—Type I/II cement (Leigh Hanson Company, Doraville, GA)—was used for all PCC samples. An ASTM standard (ASTM C150/C150M-17)[19] was followed to check the cement quality, including the 7-day strength of 2-inch mortar cubes made with cement, sand, and potable water. Coarse and fine aggregates were obtained from Augusta Quarry in Georgia (Martin Marietta, Augusta, GA). The size designations were #57 and #810 for coarse and fine aggregates, respectively. All aggregates were stored in two inside bins to attempt to maintain constant moisture states prior to batching for PCC mixtures. Physical properties of aggregates—gradation, bulk unit weight, specific gravity, absorption—were measured according to the relevant ASTM standards. The maximum size of the coarse aggregate was 1.5 inch; other properties and ASTM standards are listed in table 40.

Table 40. Physical properties of aggregates.

Item	Coarse	Fine	Specifications
Size Designation	#57	#810	ASTM C136[20]
Specific Gravity	2.4–2.9	2.4–2.9	ASTM C127[21]
Bulk Unit Wt.	110 pcf	115 pcf	ASTM C29[22]
Fineness Modulus	—	2.8	ASTM C136[20]
% Voids	30–40%	40–50%	ASTM C29[22]
Absorption	3.1–3.5%	3.0–3.3%	ASTM C128[23]

A liquid air-entraining agent (AEA) approved by GDOT was provided by Euclid Chemical (EUCON AEA-92, Euclid Chemical Company, NC) and was added to the other ingredients while they were churned in a mechanical mixer. Fly ash was also added during mixing to enhance the cementitious properties of the concrete mixture, which may help achieve the early or mid-term strength gains and possible enhancement of the PCC's resistance to

chloride ions. Two types of fly ash (Type C and Type F) were acquired from Georgia Power in Georgia and used following ASTM C618-19.[24]

PCC Mix Design

Table 41 shows a batching table containing mixture proportions and the recommended property ranges for fresh and hardened concrete samples. This mix design, designated as Class 1 GDOT standards, has been used for PCC pavements. For each batch, three quality indicators—slump, air content, and compressive strength—were closely monitored and controlled during and after sample fabrication for consistency of fresh concrete mixtures (ASTM C143[25], ASTM C231[26]) and a minimum strength requirement of 3,000 psi from 28-day moisture-cured samples (ASTM C39[27]).

Table 41. Class 1 PCC mixture design and quality control criteria.

Item	Target Value	Note	Specifications
Cement	485 lb/yd^3	Type I/II	ASTM C150[19]
Fly ash	118 lb/yd^3	Types C and F	ASTM C618[24]
Sand	1103 lb/yd^3	#810	ASTM C136[20]
Stone	1969 lb/yd^3	#57, 1.5 inch (maximum size)	ASTM C136[20]
Water	23.0 gal/yd^3	<38.4 gal/yd^3	Potable (tap water)
AEA	Variable oz	Air Entraining Admixture	ASTM C231[26]
Design air	4.7%	3.0–6.5	ASTM C231[26]
Slump	1.5 inch	0.0–2.5	ASTM C143[25]
Strength	3000 psi	28-day Minimum UCS*	ASTM C39[27]

* UCS = Unconfined compressive strength

Batching

Table 42 shows 14 mixture batches produced for the fabrication of more than 160 cylindrical samples (cylinders). The properties of these batches not only matched the mix

design variables of Class 1, but also would allow for a broader range of two key mixture variables—air content and fly ash type—that could affect the performance of PCC under some severe exposure conditions to brine.

Table 42. Mixture batch for PCC specimens.

Batch	# of Sample	Size (in)	Cement (lb)	Sand (lb)	Stone (lb)	Water (lb)	AEA (oz)	Slump (in)	Air (%)	W/C	Fly ash
1	10	4×8	10.76	24.47	43.693	5.18	0.387	0.5	7.2	0.48	C
2	15	4×8	16.46	37.43	66.81	7.93	0.092	0.3	15.0	0.48	C
3	9	4×8	10.97	24.95	44.54	7.62	0.395	1.3	5.5	0.69	C
4	15	4×8	16.46	37.43	66.81	11.43	0.610	3.3	8.7	0.69	C
5	15	4×8	16.46	37.43	66.81	10.52	0.590	1.4	9.0	0.64	C
6	15	4×8	16.46	37.43	66.81	10.52	0.427	1.5	6.1	0.64	C
7	15	4×8	16.46	37.43	66.81	10.52	0.427	2.3	12.0	0.64	C
8	15	4×8	16.46	37.43	66.81	10.00	0.427	1.3	7.5	0.61	C
9	15	4×8	16.46	37.43	66.81	10.00	0.354	1.8	8.0	0.61	F
10	14	4×8	16.46	37.43	66.81	10.00	0.000	0.8	2.0	0.61	F
11	4	4×8	5.05	11.49	20.51	3.07	0.075	0.6	7.8	0.61	C
12	4	6×12	14.82	33.69	60.14	9.50	0.089	1.1	4.3	0.64	C
13	15	4×8	16.46	37.43	66.81	10.00	0.076	1.3	4.7	0.61	C
14	15	4×8	16.46	37.43	66.81	10.00	0.050	1.1	4.0	0.61	C

The American Concrete Institute (ACI) has recognized the durability of PCC under F–T cycles should be connected to the size and volume of the entrained air bubbles (10 to 100 μm in size) in PCC.[28] These entrained air bubbles are different from trapped air pockets in size and uniformity and, more importantly, in its defense role against chloride attacks. Also, the amount of air pockets (trapped ones) is primarily affected by the water-to-cement (W/C) ratio, along with complex surface characteristics of aggregates, while the entrained air bubbles are produced only by admixtures like AEA. For batching, the initial dosage of AEA was determined in consultation with the manufacturer, but the actual

amount of air bubbles significantly changed from batch to batch to account for varying materials and environmental conditions. Individual AEA dosages were determined from the air content—a volumetric measure of all inside air—for each target level. One batch (Batch 10) was produced without adding AEA so the amounts of trapped pockets—2.0% on average—could be known. As a result, air contents ranging from 2.0% (no AEA) to 15% were introduced into different batches. Whereas most PCC samples were made with Type C fly ash, Batches 8 and 9 were prepared with Type F fly ash to explore the impact of fly ash type on the resistance of PCC to brine, as well as on the gain of compressive strength over time. Except for Batch 1, the average W/C ratios of the samples fell into a range of 0.61 to 0.69. Batch 1 is considered a trial batch, so no performance tests were conducted on it, but the entire fabrication process from batching to casting and consolidation was checked with this batch to meet the highest sample preparation standards.

PCC Sample Fabrication

After the mixture proportions were determined for each batch, PCC cylinder samples were fabricated following relevant ACI and ASTM standards (ACI 211.1-91[29] and ASTM C192/C192M–19[30]). At first, each mixture was prepared without AEA. Then, a proposed amount of AEA was added to the premixed batch and then thoroughly mixed for another 5–10 minutes with a mechanical mixer (Proforce, 110 lb, 25 rpm) to ensure the air bubbles were well dispersed throughout the batch. If the target air content was not met with the initial AEA quantity, this process was repeated with an adjusted AEA dosage. After the mixing process, the terminal slump and air content were recorded before the final mixture batch was cast and consolidated in plastic molds to form concrete cylinders. There were

two sample sizes: 4 inches in diameter by 8 inches in height (4×8 inch) and 6 inches in diameter by 12 inches in height, (6×12 inch). The consolidation process was facilitated with an internal vibrator to ensure and maintain as few trapped air pockets as possible. After the consolidation, all 4×8-inch concrete molds were put into a curing chest where both temperature and moisture were controlled. After 7 days of curing, plastic molds were removed, and concrete cylinders were put back into the moisture-controlled curing boxes to be cured for another 21 days or until they were used for testing. Figure 34 shows 4×8-inch cylinders being cured in a moisture-controlled box. The sample identification code marked on each sample reveals both batch number and sample number (e.g., 5-4 means the fourth sample in Batch 5).

Figure 34. Photo. Four-inch-diameter concrete cylinders in moisture curing box.

Each 6×12-inch cylinder was cast with an EC dowel bar for the corrosion investigation of EC dowel bars. GDOT provided eight EC dowel bars that are 1.5 inches in diameter and either 18.5 inches or 16 inches in length. Figure 35 shows the dowel bars. The dowel bars were all well coated with epoxy except for the ends of each bar, and they met the requirements stated in AASHTO M254.[31] Each dowel bar was positioned at the center of the cylinder for the corrosion test to allow simulation of three migration paths of brine toward the dowel bar in PCC pavement: direct exposure at the uncoated end, direct exposure on the fully coated body (near the cylinder top), and the concrete surface to core. To center the dowel bar in each cylinder, both the top lid and the bottom of the mold were designed to hold the position of a dowel bar during casting and consolidation. All 6×12-inch cylinders were cured in a separate dry curing box to prevent rust from forming at the ends of the dowel bars. Figure 36 shows the plastic mold and concrete cylinders with dowel bars after 28 days of curing.

Figure 35. Photo. EC dowel bars for corrosion test.

Figure 36. Photos. Plastic mold (left) for 6×12-inch cylinders with dowel bars (right).

Experimental Programs

28-day Compressive Strength

The compressive strength of the 28-day samples was measured using a hydraulic loading machine with a maximum capacity of 300,000 lb (Humboldt). For the 10 mixture batches (Batches 1 through 10 listed in table 42), three samples were selected from each batch and were fractured in a uniaxial mode.

The strength data collected from different batches will be used to explore the impact of two design variables—air content and fly ash type—on the compressive strength of PCC cylinders cured for 28 days and longer. Also, the effects of brine on the compressive strength can be explored and correlated with other performance indicators. Figure 37 shows the compressive strength test of two samples from Batch 5.

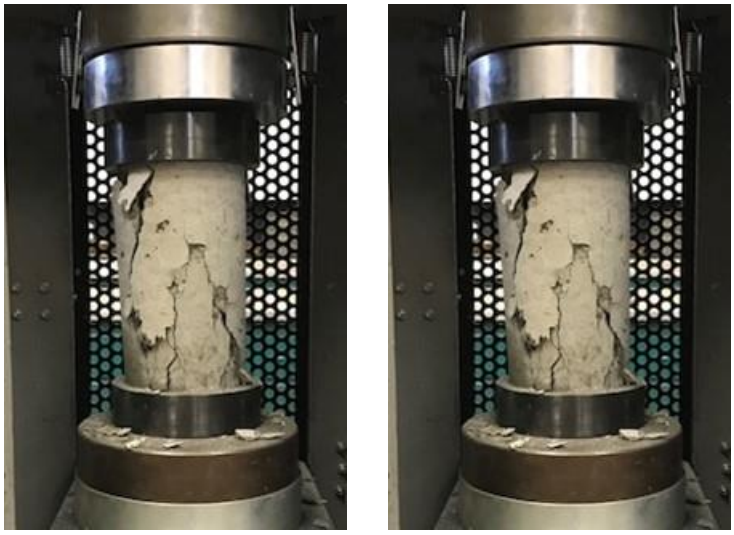

Figure 37. Photo. Compressive strength test (sample no. 5-3 and 5-6).

Ambient Erosion Test

Conventional durability tests that involve wetting and drying (W–D) cycles might be less appropriate for simulating brine damages in PCC near pavement joints or existing cracks. During the winter, those vulnerable areas are prone to a constant saturation due to frequent anti-icing operations, often combined with pre-wetting of rock salt. Also, most of the W–D cycles are applied to PCC samples at preselected temperature changes, which cannot reflect the real field temperatures.

In this study, the researchers designed an ambient erosion test that aims to mimic the concrete near the pavement joint that is subjected to a constant attack of brine. All erosion tests were conducted at air temperatures from January 2020 to September 2020 and may be continued beyond the project period. PCC samples from several batches were selected for this experiment. Six 4×8-inch cylinders from each batch were weighed and then soaked in the buckets of brine solutions—one sample per solution concentration—immediately

after their 28-day curing period ended. Figure 38 shows the samples in brine buckets prepared for the ambient erosion test.

Figure 38. Photo. Ambient erosion test setup.

Prior to the test, the damage potential of each sample was characterized by the level of resistance of PCC to chloride ion penetration, as measured by the surface resistivity tester. As described further in the Results section of this chapter, the surface resistivity of PCC can indicate its durability when subjected to chloride ions and reflect the impact of some properties of PCC across the design variables. Every 2 weeks, all samples were taken out of the buckets, thoroughly washed with tap water, and air-dried before their weights were measured on a scale. Then, the surface resistivity of each sample was measured and recorded before putting it back into the bucket. This testing schedule was maintained prior to being severely interrupted by a university-wide closure due to the COVID-19 pandemic. Combined with other test results, the findings of this test will offer some meaningful insights into the different damaging effects of brine solutions on PCC, leading to the

recommendation of an optimum range of brine concentrations that would be less damaging to PCC pavement and yet still be effective in preventing any significant snow and ice accumulation.

Surface Resistivity Test

Resistivity is the electrical resistance of a substance, normalized to a unit cross-section and length, and is the reverse of conductivity. In concrete, the resistivity measured at the surface, i.e., surface resistivity (SR), can be interpreted as an ability of concrete to resist the penetration of chloride ions that constitute brine solutions commonly applied in Georgia. This study employed the Wenner probe technique to measure the chloride ion diffusivity in hardened concrete samples that is linked to the level of resistance of PCC to brine. This technique was developed originally by Wenner at the National Bureau of Standards in the 1910s in the geology field to determine soil strata, and it was then modified over time for a concrete application. The applications of the Wenner probe in PCC experiments have expanded noticeably since the work by Morris et al. in 1996.[32] In this technique, four equally spaced linear electrodes are used to measure the SR of concrete (figure 39).

The two external electrodes apply an alternating current (AC) to the concrete surface, while the electrical potential is measured from the internal probes. It should be noted that direct current (DC) is not desirable as it may result in inaccurate readings because of the polarization effect. To measure the surface resistivity, AASHTO TP 95-11[33] is the only specified standard that requires an electrode spacing of 1.5 inches (or 38 mm) with an AC

frequency of 13 Hz.[33] When the sample thickness is much greater than the distance between the points, the SR can be estimated as in equation (2).

$$SR = 2\pi dP°/I \quad (2)$$

Where,

SR = *SR* reading at one location

d = distance between points (electrodes)

P = measured potential

I = applied current

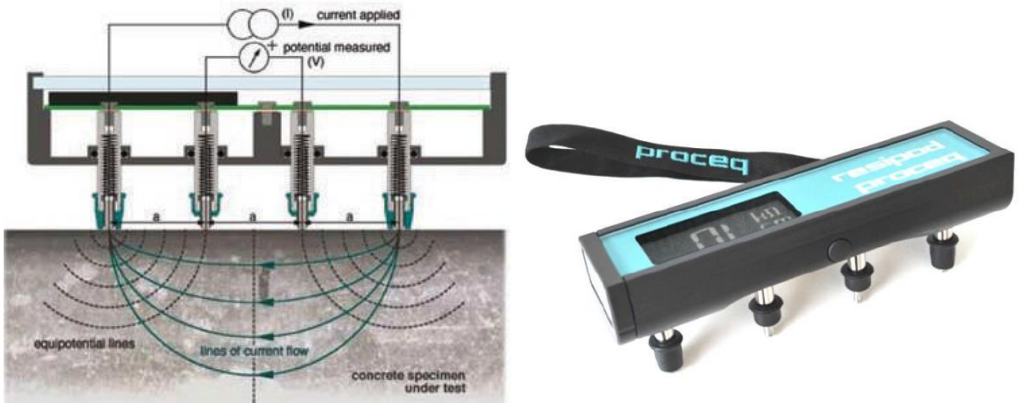

©Proceq

Figure 39. Illustration. SR test and apparatus (courtesy of Proceq).

Each SR value indicates the average reading taken at four different locations, aligned at 0°, 90°, 180°, and 270° circumferential marks on the longitudinal side of the sample. According to ASTM C1556 [34], the chloride ion permeability becomes high (or very likely) when the SR value is smaller than 12 KOhm-cm for 4-inch samples. Table 43 shows the target permeability levels associated with the SR values.

Table 43. Chloride ion permeability based on SR value.[34]

Chloride Ion Penetrability	Surface Resistivity Test (KOhm-cm)	
	4×8-inch Cylinder	6×12-inch Cylinder
High	<12.0	<9.5
Moderate	12.0–21.0	9.5–16.5
Low	21.0–37.0	16.5–29.0
Very Low	37.0–254.0	29.0–199.0
Negligible	>254.0	>199.0

Several laboratory and field studies have included SR tests. In Florida, Kessler revealed that the SR test can offer an indicator of chloride penetration resistance at 28 days for concrete samples that have reached a large portion of their total reaction, such as those produced with silica fume or metakaolin.[35] Vivas et al. conducted a rigorous study comparing SR measurements to bulk diffusion, rapid chloride permeability measurements, and quick migration test results.[36] They showed that a good correlation exists between all test methods at various ages of testing, with the best correlations existing between the 91-day rapid chloride permeability and the 364-day bulk diffusion test results. A similar study conducted by Rupnow and Icenogle reported that SR measurements correlate well with rapid chloride permeability measurements across a wide range of permeability values and sample testing ages.[37] Good correlations were found to exist between both the 14-day and 28-day SR values and the 56-day rapid chloride permeability values. Also, the SR value was able to identify significant differences in W/C ratios for the same mixtures. Compared to the rapid chloride permeability test, a vast amount of cost savings can be achieved by implementing the SR technique for quality acceptance and control. Presuel-Moreno et al. characterized over 60 bridges in Florida using the SR test method.[38] Their results showed that a correlation existed between samples tested in field conditions (i.e., non-saturated) and samples taken to the laboratory and subsequently tested in a wet (i.e., saturated)

condition. The correlation showed that the field SR was generally three times that of the wet condition samples. Of course, the SR test has some drawbacks. For instance, steady-state conditions are challenging to achieve during the test, and thus a more detailed analysis should be required.[39]

These previous works offer some lessons. Primarily, multiple validations of SR tests allow this study to be conducted without resorting to the rapid chloride permeability tests that cost so much more than SR tests. SR tests could be suitable for the proposed ambient erosion test where the saturation level is relatively constant during the measurements compared to the F–T tests. Typically, PPC samples with a higher percentage of air bubbles result in lower SR values. Since lower SR values indicate higher permeability of chloride ion, this implies that PCC with higher voids is more vulnerable to brine-driven damages. However, this reasoning is not as sophisticated as needed because of the pore structure changes under numerous design factors. Sample age would be one of the influential factors in that process. So, with SR tests, the impact of brine concentration will be investigated with PCC samples conditioned for the ambient erosion tests. The correlation of SR values of laboratory PCC samples with those of field samples would be beyond the scope of this study and must be investigated through more comprehensive efforts.

Rapid Freeze–Thaw Tests

Focusing on F–T damages in concrete, another laboratory testing program was devised from ASTM C666/C666M[40] to simulate the rapid degradation of PCC samples under the combination of brine and extreme temperature cycles. To this end, a chest freezer capable of reaching -40°C (FDC-4000, SO-LOW, Bridgeview, IL) was modified with a

temperature-control system. This system allows for the PCC samples to be continuously heated and cooled—across the freezing point—inside the freezer while being soaked in small individual containers filled with brine solution. Figure 40 shows the freezer fitted with the temperature-control system.

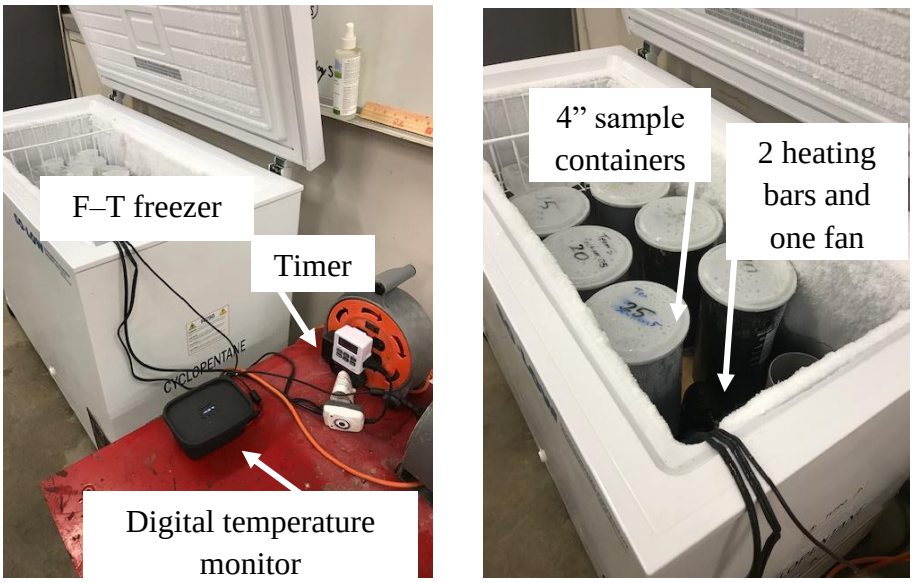

Figure 40. Photo. Chest freezer with temperature-control system for F–T test.

One F–T cycle was set to complete in a day and 10 F–T cycles constitute most rapid F–T tests, but more F–T cycles were applied to the PCC samples from Batch 9 (30 cycles) to understand the longer-term performance of PCC samples. The F–T tests usually continue for the given PCC sample either until it has been subjected to 300 cycles or until its relative dynamic modulus of elasticity (MOE) reaches 60 percent of the initial modulus. However, this study found that some longitudinal moduli drop more than 60 percent even after the first 10 F–T cycles. This might be attributed to the impact of the brine effects. Hence, the 10 F–T cycles were maintained unless more F–T cycles are deemed necessary for a long-

term characterization. Due to the capacity limits of the freezer, only six samples were conditioned and tested simultaneously during the F–T tests. Testing conditions were monitored continuously and checked to ensure whether the peak temperatures (+1°C and −16°C) were reached at specified rates within a cycle, and uniform temperature cycles were maintained for the entire F–T set (10 cycles or 10 days). Based on the suggested F–T testing procedure, the total thawing time must be less than one-quarter of the freezing time. The timing for the thaw cycle was therefore set to 6 full hours, and the temperature within the freezer was controlled to as close to the recommended standard as possible.

The temperature inside the freezer was measured with a microcontroller fitted with a temperature probe that extends into the freezer chest. Although the freezer does include its own temperature-control mechanism, that internal temperature-control mechanism does not allow for data logging. The temperature reading was obtained approximately every 15 minutes to ensure an appropriate resolution of temperatures were obtained throughout each testing day. The temperature data were then stored on an SD memory card, allowing for retrieval for observation and analysis.

During the thaw cycle, two means of heat were supplied to the freezer. A heating bar was used to heat the liquid bath inside the freezer, and a heated air blower was used to provide even distribution of heat via convection inside the freezer. This combination of heat distribution system was timed to increase temperature for the thawing cycle, and once the thawing cycle ended, the freezer would proceed to lower the temperature. A sample plot of the F–T cycle for a 1-week duration is shown in figure 41.

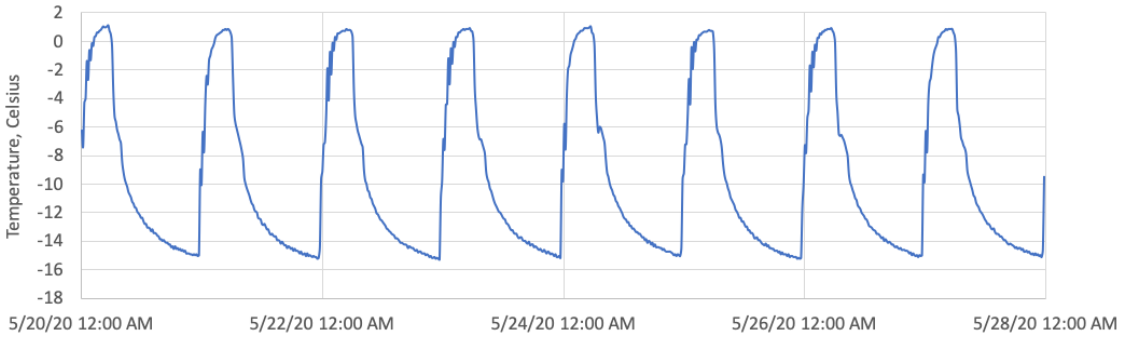

Figure 41. Graph. Temperature cycles for 8 days of F–T test.

Impact Resonance Tests

To characterize the PCC under various exposure conditions, the modulus of PCC samples was selected as the primary performance indicator. Compared with conventional strength tests, which are destructive, the modulus can be continuously measured and monitored with the least interference with the degradation process of the PCC samples. In accordance with ASTM C215[41] and ASTM C666/C666M[40], the dynamic Young's moduli of elasticity (or dynamic moduli) and the relative dynamic modulus were calculated from fundamental frequencies measured with an impact resonance (IR) apparatus (RTG-1, Olson Instruments, Inc). Figure 42 shows the IR test system, which includes a laptop computer with data collection and processing software, a small hammer to impact the concrete specimen, an accelerometer to measure the vibration response of the concrete sample, an accelerometer cable, a mounting block, adhesive, and a foam pad for specimen support.

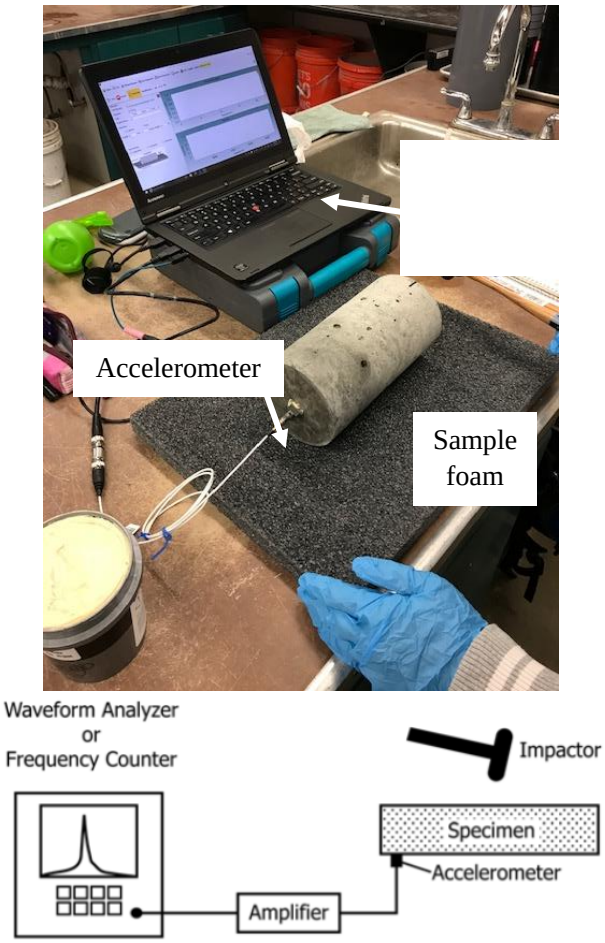

Figure 42. Photo and Illustration. Impact resonance apparatus (RTG-1, Olson Instruments, Inc).

Every IR test involves striking a concrete specimen with a small ball-peen hammer and measuring the resulting vibration energy with an accelerometer mounted on the sample. The time-domain acceleration response is temporarily recorded and then converted into the frequency domain to detect the resonant frequency with the embedded fast Fourier transform (FFT) algorithm. The resonant frequencies are a function of the specimen geometry and material properties and are collected from different accelerometer attachment points and hammer strike locations to define three resonant frequencies: transverse, longitudinal, and torsional. These fundamental frequencies, along with

dimensional and material properties of a PCC sample, can be used to calculate the corresponding dynamic moduli and the relative dynamic modulus as seen in equation 3 through equation 6.

$$\text{Transverse Dynamic Modulus} = CMn^2 \quad (3)$$

where, M = mass of specimen in kg; n = fundamental transverse frequency in Hz; and $C = 1.6067\ (L^3T/d^4)$ in m^{-1} for a cylinder, where L = length of a specimen in m, d = diameter of the cylinder in m, and T = correction factor that depends on the ratio of the radius of gyration and on Poisson's ratio.

$$\text{Longitudinal Dynamic Modulus} = DM(n^2) \quad (4)$$

where, n = fundamental longitudinal frequency in Hz, and $D = 5.093\ (L/d^2)$ in m^{-1} for a cylinder.

$$\text{Torsional Dynamic Modulus} = BM(t^2) \quad (5)$$

where, t = fundamental torsional frequency in Hz, $B = (4L/A)$ in m^{-1}, and A = cross-sectional area of test specimen in m^2.

$$P_c = (f^2/f_1^2)/100 \quad (6)$$

where, P_c = relative dynamic modulus of elasticity, after c cycles of freezing and thawing, in percent; f = fundamental transverse frequency at 0 cycles of freezing and thawing; and f_1 = fundamental transverse frequency after c cycles of freezing and thawing.

During the IR tests, the hammer impact was made multiple times (7 to 10) for each sample. The interquartile range rule—a descriptive statistical measure of variability—was employed to detect outliers and to define representative frequencies during the data process.[42]

The structural degradation of PCC, especially during the rapid F–T tests, can be characterized by the relative dynamic modulus in equation (6). The results exhibit how the relative dynamic moduli of brine-treated PCC samples would change after the first 10 F–T cycles, suggesting a varying impact of brine solutions on PCC pavement under the worst potential climatic conditions in the State.

Resistance of EC Dowel Bar to Corrosion

The performance of EC dowel bars in PCC pavement during the winter is one of the major concerns to GDOT even though the effectiveness of epoxy-coated bars in preventing corrosion has been well demonstrated in the literature. The experimental program of this study is aimed at understanding if different migration paths of brine solution onto the dowel bar can make a difference in its corrosion resistance. To this end, four 6-inch cylinders (Batch 11) fabricated with dowel bars were prepared and treated with four types of brine solutions (B-0, B-5, B-10, and B-15 in table 39). The brine treatment involves soaking each sample in a respective brine solution for 24 hours, followed by covering the cylinders with plastic wrap to minimize any excessive evaporation. The corrosion tests were run on two distinct conditions: F–T cycles and dry in the air, as shown in figure 43.

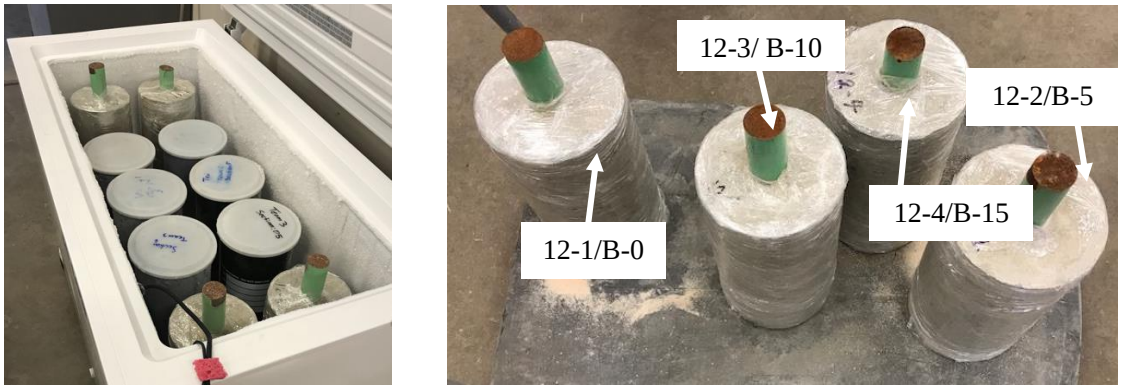

Figure 43. Photos. Six-inch dowel bar samples in F–T (left) and air-dry conditions (right).

For the first 86 days (March 24 to June 18), with minimal interruptions, the prepared 6×12-inch samples underwent F–T cycles in the freezer alongside the other short-term F–T tests for the 4×8-inch samples. Soon after those multiple F–T cycles, the dowel bar samples were taken out of the freezer and placed on the floor of the laboratory for another 85 days (June 18 to September 11) during which brine continuously affected the concrete and dowel bars in a dry condition.

This testing program was developed to hopefully simulate the field conditions that dowel bars might experience during the warm and cold seasons. These test methods do not account for W–D cycles, especially at higher temperatures (e.g., wet at 23°C and dry at 37.7°C) adopted in a recent FHWA study.[43] Also, the results of the test are reported based on visual inspection only, not by sophisticated corrosion-level measurements such as macro-cell corrosion current density, the instantaneous rate of corrosion, or AC resistance data.

RESULTS

Effect of Design Variables on Compressive Strength

Figure 44 displays the average 28-day compressive strength obtained from three 4×8-inch cylinders randomly chosen from each of 10 batches (Batch 1 through Batch 10). Batches 2 and 7 do not meet the strength requirement (3,000 psi), likely due to high air void contents: 12% and 15%, respectively. In contrast, samples from Batch 10 (2.0% air), where no AEA was added to the mixture, resulted in the highest strength gain. This clearly shows that air content can be one of the dominant factors affecting strength gain, whereas other design variables play a minor role in gaining strength over time.

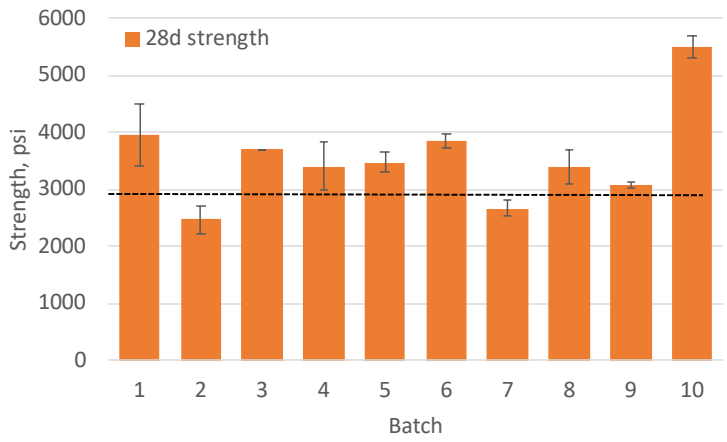

Figure 44. Graph. 28-day average compressive strength of PCC samples.

To evaluate the potential role of compressive strength as an indicator of F–T damages, additional strength tests were performed before and after the rapid F–T tests. Six concrete cylinders were collected from each of three batches (Batches 6, 8, and 10) for this investigation, but only samples from Batch 10 were fractured before the F–T cycles due to the limited capacity of the freezer and testing schedule conflicts. As seen in figure 45, the

strength even after the rapid F–T test was higher than that of the 28-day strength as concrete samples continuously gain their strength over time in moisture conditions. Data from Batch 10 illustrate that the damaging effect of F–T cycles could be detected and quantified with the drops in strength data after the F–T tests. Similar observations could have been made in Batches 6 and 10 if strength data were available for these batches long after 28 days but before the application of F–T cycles. However, it should be noted that strength data alone would not be appropriate either to characterize F–T damages or to evaluate the impact of brine solution on PCC when the level of damage (i.e., strength drops) is too small compared to the amount of strength gain. When this level of damage occurred during the rapid F–T cycles, the IR tests seemed better able to capture the impact of the brine solution on PCC, as well as to quantify the evolution of the structural integrity.

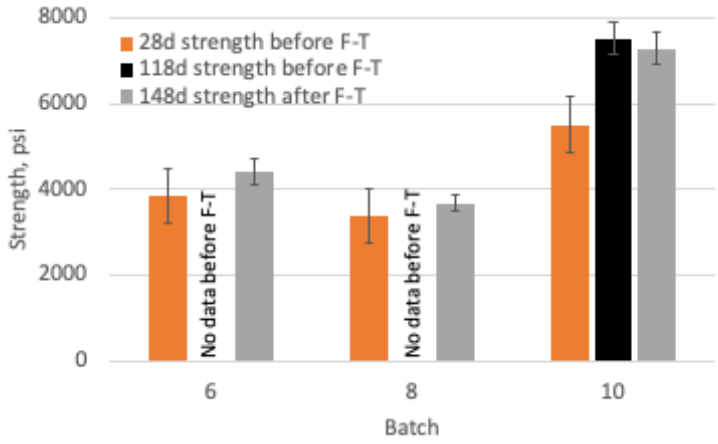

Figure 45. Graph. Strength variation after F–T test.

Effect of Design Variables on Surface Resistivity

The development of the internal structure in PCC during the hydration process is deeply affected by the formation of a pore structure, especially at an early stage. Similarly, the

strength gain in this phase can be associated with the amounts of internal voids, as demonstrated in the previous section, Research Method. Since the SR tests are conducted to measure the electrical potentials that are sensitive to the pore structure of PCC, the resulting SR values may be used as strength indicators. To prove this hypothesis, an experimental attempt was made by correlating the SR values with the strength gains in PCC. Figure 46 shows the SR values (or resistivity) collected from multiple batches on two selected curing days, including the 28 days. These samples have never been subjected to a brine solution and were only moisture-cured during the test.

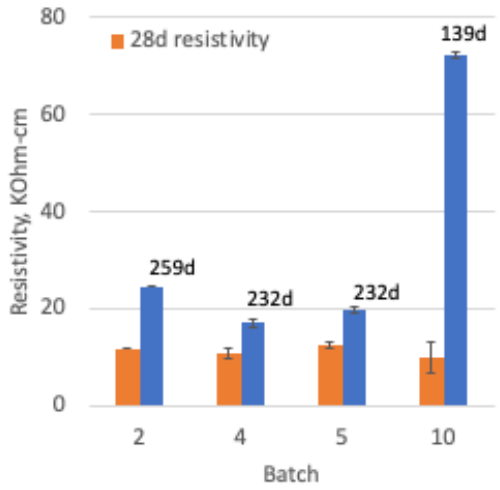

Figure 46. Graph. IR values of PCC sample.

Clearly, the resistivity variations between batches closely match the characteristics of strength gain already seen in figure 44 and figure 45. Batch 10 exhibits the highest increase in SR values, which is consistent with the highest strength gain in the same batch due to the least amount of air contents. Batches 4 and 5 reveal similar SR values on both curing days. However, samples from Batch 2 show a higher increase in SR values than Batches 4 and 5, suggesting faster strength gain despite the higher air contents (15%). It would be

plausible for the SR tests to be used as a strength monitoring tool for intact PCC samples. However, caution must be exercised when the data are translated into the field performance of PCC, as it will be subjected to various levels and durations of exposure conditions.

Effect of Brine Concentration on PCC's Resistance to Chloride Ion

The SR data were collected from PCC samples treated with brine for the ambient erosion tests and were analyzed to understand how PPC's resistance to chloride ions varies with brine concentration. This investigation also focused on the contributions of air contents and fly ash types (C and F) to the chloride ion permeability. Figure 47 shows the SR values of samples collected from Batches 2, 3, 5, and 9 that have been thoroughly saturated in brine solutions (B-0 to B-25). Following the procedure for the ambient erosion test, all the samples were put into the brine buckets as soon as they turned 28 days old. The terminal resistivity was collected at slightly different days due to the staggered sample fabrication schedule, but the long-term effects of both air content and brine concentration were well captured. Any SR value smaller than 12 KOhm-cm implies high permeability for the tested sample geometry, according to ASTM C1556.[34]

First and foremost, samples in higher brine concentrations—greater than 15% $CaCl_2$ (B-10)—are expected to suffer the most damages from chloride permeability, whereas lower brine concentrations, such as B-0 and B-5, appear to have a low (21–37 KOhm-cm) to moderate (12–21 KOhm-cm) impact. On the other hand, it is interesting to note that type of fly ash influences the vulnerability of PCC to chloride attack, and between the two fly ash types tested, the Type F was pronounced an effective deterrent to chloride ion permeability, especially at 0% $CaCl_2$ (B-0). However, this effect quickly fades away at higher concentrations.

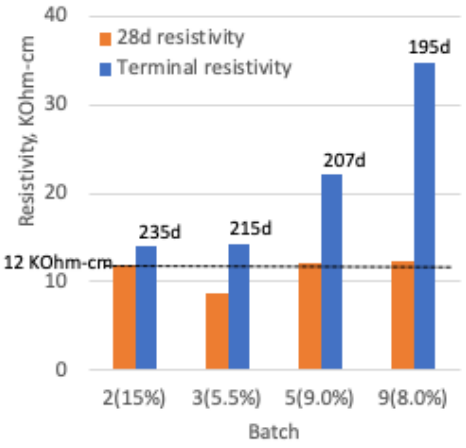

(a) B-0

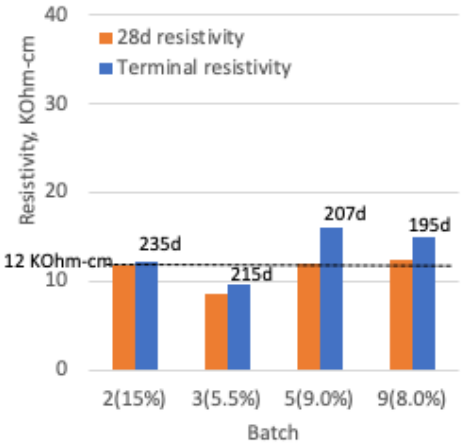

(b) B-5

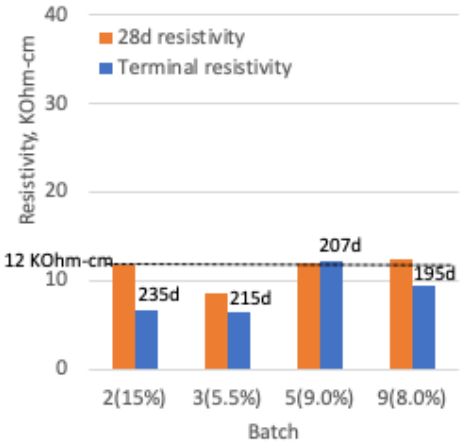

(c) B-10

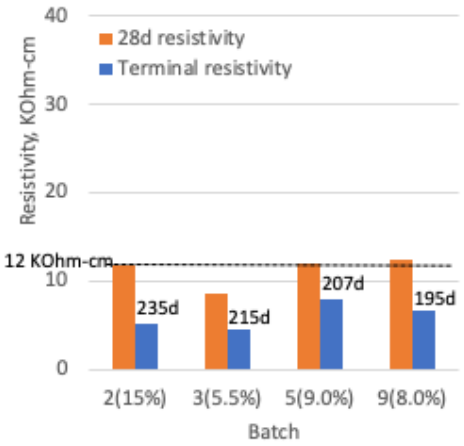

(d) B-15

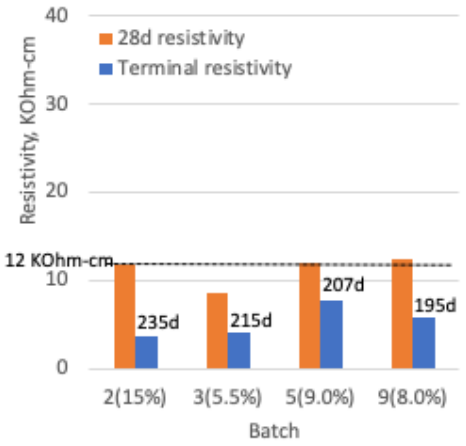

(e) B-20

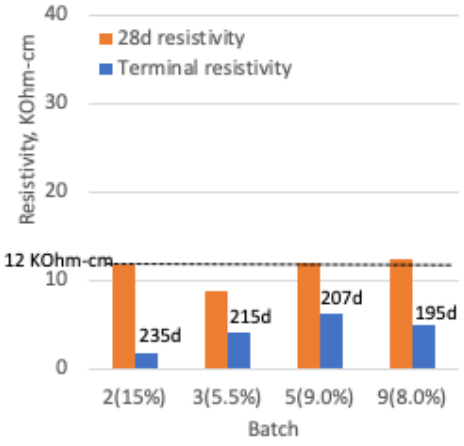

(f) B-25

Figure 47. Graphs. Impact of air content on SR value for different brine concentrations.

The role of air content in resisting chloride ions is not as conspicuous. Both Batch 2 (15% air content) and Batch 3 (5.5% air content) perform almost the same in B-0, but as the concentration increases, both batches fall into the high-risk zone. The likelihood of being damaged looks higher in Batch 2 than in Batch 3. A current design requirement for Class 1 mixture specifies an air content range of 3.0–6.5%, which makes Batch 3 (5.5%) acceptable. However, a bit higher air contents than 6.5% might be beneficial for PCC pavement to be resistant to chloride ions at lower concentrations (B-0 and B-5) according to the results. It is worth noting that these findings are based on the simulated field conditions where no significant F–T damages are anticipated but can be applicable for some regions in Georgia that would experience longer mild temperatures after multiple brine treatments, often combined with pre-wetting operations.

Impact of Brine on F–T Damage of PCC

The damage in PCC pavement can be accelerated with F–T cycles when brine is applied. To simulate these conditions in the laboratory setting, concrete cylinders from three batches (Batches 6, 9, and 14) were used for the rapid F–T tests. These batches cover an air content range of 4.0–8.0%. Excessively high air contents (above 10%) were not included in this experiment due to the lack of proven benefits for the prevention of brine damages. From Batch 6, two sets of samples (12 cylinders in total) were prepared: one set with a pretreatment of brine for 5 weeks in brine buckets; the other group with no prior treatment with brine before F–T cycles. Samples from Batch 9 underwent three sets of rapid F–T tests (10 F–T cycles in each set), whereas only one set of F–T cycles was applied to the other batches. Table 44 lists the relative dynamic moduli calculated from the transverse frequencies using equation (6). With the IR testing system, transverse frequencies were

measured before and after the F–T tests. The relative dynamic modulus indicates the percent changes between two transverse frequencies, and a higher dynamic modulus means less damage (or structural degradation). The average dynamic moduli suggest that, overall, samples conditioned with low brine concentrations (B-0 and B-5) display more F–T damages compared to higher concentrations. However, in Batch 6 (6.0% air), the effect of B-25 (25% $CaCl_2$) was found to be equally damaging with lower brine concentrations. It is worth noting that the effect of air content on dynamic modulus in PCC is pronounced in Batch 6 (6.1% air) and Batch 14 (4.0% air). Both batches are made with AEA, so those samples can benefit from the entrained air bubbles when resisting the brine attacks. However, it seems that the lower air contents in the design range (3.0–6.5%) can still offer a proper defense. In Batch 6, the effects of the pretreatment on the dynamic modulus were not clearly shown, except that samples became more prone to damages at higher brine concentrations after the pretreatment. Despite the higher air content (8.0%) and multiple F–T cycles, samples mixed with Type F fly ash (Batch 9) performed well across the brine concentrations, which is reasonably consistent with other favorable effects on compressive strength and resistivity to brine (SR value).

Table 44. Relative dynamic modulus for batches 6, 9, and 14.

Batch No	Relative Dynamic Modulus, Percent									
	Brine Concentration, Percent						Fly ash	Pre-treatment	No. of F–T Cycle	Air Content
	0	5	10	15	20	25				
6	89.8	99.1	96.5	93.6	93.8	91.1	C	Y	10	6.1%
	86.4	84.3	87.5	99.8	96.3	92.7		N	10	
9	88.3	92.2	92.8	95.0	98.0	96.1	F	N	10	8.0%
	91.5	91.9	93.8	96.5	96.1	97.6			20	
	92.1	91.8	93.8	96.8	96.4	97.7			30	
14	94.3	94.5	97.8	95.1	95.0	98.9	C	N	10	4.0%
Average	90.4	92.3	93.7	96.1	95.9	95.7				

Effect of Brine and F–T Cycles on Scaling Potential in PCC

As one of the forms of physical damage in PCC, surface scaling (i.e., salt scaling) is quite common in concrete pavement. Despite its minor impact on structural degradation, this phenomenon often leads to the acceleration of chloride ingression and frost damages. There are several mechanisms proposed to explain the initiation and propagation of scaling in PCC, such as thermal shock, precipitation and growth of salt crystals, hydraulic pressure, and glue spalling.

To evaluate the scaling potential in PCC subjected to both brine and F–T cycles, concrete from samples from Batches 7, 13, and 14 were collected from the F–T tests and visually inspected for any evidence of surface scaling. These samples underwent the same conditions as those used for the IR characterizations but were reserved for this line of investigation. Figure 48 shows the concrete samples, which exhibit a varying degree of scale damages.

Batch 7 (Sample ID 7-10 to 7-15)

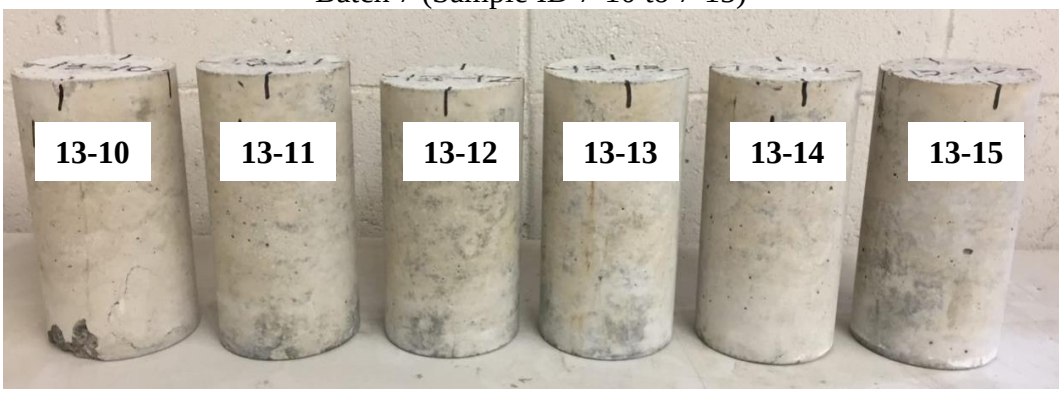

Batch 13 (Sample ID 13-10 to 13-15)

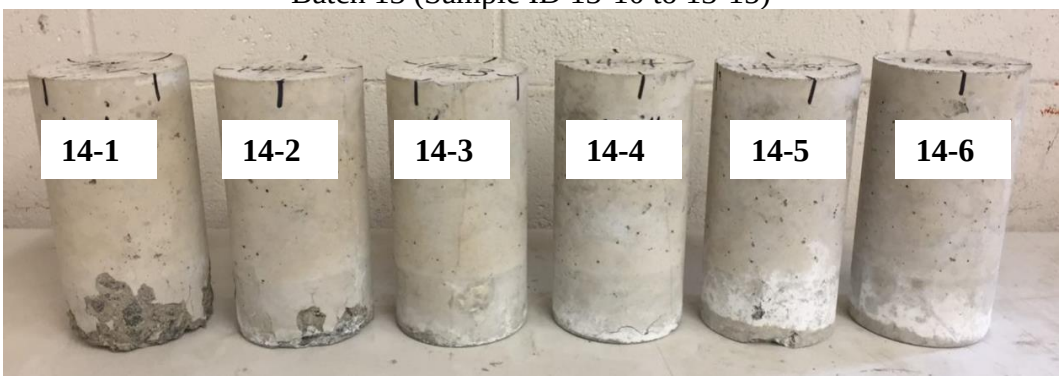

Batch 14 (Sample ID 14-1 to 14-6)

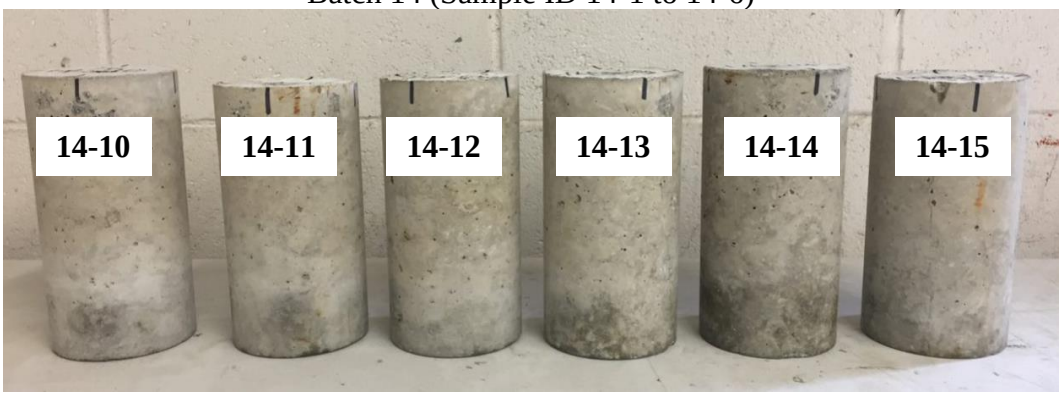

Batch 14 (Sample ID 14-10 to 14-15)

Figure 48. Photo. PCC samples used for inspection of surface scaling.

Batch 13 (13-10 to 13-15) and Batch 14 (14-1 to 14-6) contained the most severely scaled spots, while other samples revealed almost no visible scaling, having only some sporadic white marks and shadow. It should be noted that PCC samples treated with lower brine concentrations (B-0 and B-5) seem more vulnerable to scaling. This agrees well with one of the findings in the IR study, where the relative dynamic modulus becomes smaller at lower brine concentrations.

As several scaling mechanisms imply, scaling is triggered by multiple internal (e.g., pore structure and air content) and external (e.g., F–T cycle and brine concentration) causes, not by a single dominant one. So, the potential of surface scaling can vary even in the same sample batch. No scaled spots were observed from samples 14-10 to 14-15, whereas severe scaling was seen in samples 14-1 to 14-6. For that reason, it is hard to confirm that the lack of scaling in Batch 7 is due to the higher air content (12%).

The changes in the sample's weight were measured after the F–T tests to support the visual observations. As table 45 shows, on average the percentage weight loss was higher at lower brine concentrations (B-0 and B-5), suggesting the weight loss should be associated with the scaling potential to some degree. Except for B-0, the weight loss in Batch 7 appears comparable with that of the samples from Batch 14.

Table 45. Weight loss of sample after F–T test.

Batch	Sample ID	Weight Loss, Percentage					
		Brine Concentration, Percentage					
		0	5	10	15	20	25
7	7-10 to 7-15	1.656	1.573	1.575	1.355	1.418	1.551
13	13-1 to 13-6	1.137	0.964	0.967	0.992	1.019	1.019
14	14-1 to 14-6	2.488	1.562	1.303	1.242	1.295	1.314
	14-10 to 14-15	0.275	0.439	0.332	0.491	0.625	0.530
	Average	1.389	1.134	1.045	1.020	1.089	1.104

Corrosion Resistance of EC Dowel Bar

After completing the programmed cycles (86 days of F–T cycles and 85 days of air-drying in the laboratory), a simple forensic study was conducted on the samples to visually detect any corrosion of the dowel bars. To remove the concrete cover without causing any mechanical damage to the dowel bar, splitting tensile loading was applied, as shown in figure 49.

Figure 49. Photo. Removal of concrete from corrosion sample.

Figure 50 shows the conditions of the EC dowel bars taken out of the cylinders. Several spots showed some coating damages caused either by sharp edges of the cylinder or by pointed aggregates in the concrete during removal, but overall, the dowel bars maintained their pristine condition. A careful inspection of the dowel bars led to the conclusion that there was no evidence of corrosion except for the uncoated ends where the dowel bars had been in direct contact with brines during the test.

Figure 50. Photo. Dowel bars after corrosion test.

The corrosion levels are not distinguishable and not in proportion to the brine concentration. This result is consistent with what a recent FHWA study[43] found about the EC dowel bars. However, the test proposed and conducted in this study lacks some experimental sophistications, mainly due to the limited testing resources. Therefore, a comprehensive study must be designed and conducted to validate the current findings under a broader spectrum of testing conditions, including W–D cycles at higher temperatures.

Recognizing this, researchers at Kennesaw State University (KSU) have recently redesigned the specimen geometry to better simulate joint conditions in field PCC pavement, although this is unlikely to be part of the current study. Figure 51 shows KSU's new concrete form built to cast "joint samples." On each dowel bar, three pits (i.e., 3/8-inch holes drilled into the body) were made to initiate corrosion, as one of the pits in the middle would sit 0.5-inch below the bottom of an artificial joint. As for the testing conditions, F–T cycles were no longer necessary, as corrosion prefers warm and humid conditions. A temperature chamber capable of controlling temperatures between 20°C and 40°C would be an essential tool for this new experiment.

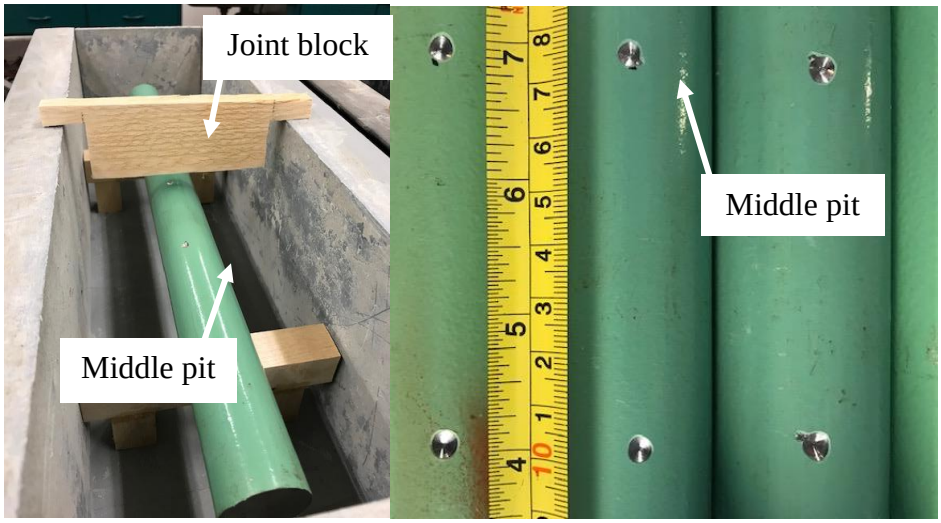

Figure 51. Photo. Plastic mold for joint samples with wood chairs (left) and dowel bars with pits (right).

CHAPTER 5. SUMMARY, CONCLUSIONS, AND RECOMMENDATIONS

SUMMARY AND CONCLUSIONS

This research aims to optimize the winter treatment operations and specially to minimize the impact to Georgia pavements. This project investigated the efficiency of two typical deicers (i.e., sodium chloride and calcium chloride) that are commonly used by GDOT to treat pavement surfaces during the winter season. The effect of these deicers on the performance of asphalt binders and Portland cement was evaluated. The following conclusions can be drawn:

1. The 23% NaCl brine prepared with GDOT rock salt had a measured freezing point of 3.2°F (−16°C). The freezing point of the brine decreased when additional calcium chloride was added into the 23% NaCl brine. The measured freezing point of the blended brine ranged from 2.2°F (−19°C) with 5% $CaCl_2$ to 20.2°F (−29°C) with 25% $CaCl_2$. In general, the measured freezing points from GDOT salts were slightly higher than the pure salt brines due to the impurity of the GDOT salts.
2. The measured freezing points of the blended salt brines were slightly different from the calculated values from the theoretical equation. A regression equation was calibrated from the test data, which can be used to calculate the freezing point of blended brines prepared with GDOT salts.
3. Blended brines of calcium and sodium chlorides demonstrated some capacity to penetrate ice (for deicing) at 25°F (−3.9°C). The capacity decreased quickly with a decrease in temperature and showed very limited penetration to the ice at temperatures of 15°F and below.

4. Blended solid deicers of sodium and calcium chlorides were more effective and economical than using rock salt alone when the temperature was below 2°F (−16.7°C). As the temperature increased, there existed an optimum blend ratio of calcium chloride to achieve the lowest material cost. When the temperature was above 20°F (−6.7°C), it was not necessary to use calcium chloride in the solid deicer, as it increased the material cost. At medium temperatures of 2°F (−16.7°C) to 20°F (−6.7°C), the optimum mixing ratio of calcium chloride was around 0.05 to 0.15 per part of sodium chloride.
5. The retention rate of the brine on the road surface depended on the pavement smoothness. The measured retention rate from OGFC, Superpave, and Portland cement concrete pavements were 97, 92, and 77 percent, respectively. The retention rate reduced when the grade of the pavement surface exceeded 10 percent. However, the effect was negligible when the surface grade was less than 10 percent. Further, the retention rate of the brine was higher on dry pavements than on wet pavements.
6. The rheological property at high temperatures, $G^*/\sin(\delta)$, of original binders and RTFO residuals after soaking was observed to increase slightly regardless of the duration of soaking, indicating the rutting resistance of the tested binders was not negatively affected by soaking. There was a significant difference of $G^*/\sin(\delta)$ caused by the type of binder, i.e., the unmodified binders were more sensitive to soaking in brines.
7. The $G^*\sin(\delta)$ at intermediate temperatures was slightly increased in general after being soaked in the brine of 23% NaCl, and then decreased with continued addition

of calcium chloride. The differences of increase and decrease in G*sin(δ) were, however, insignificant with regard to the type of binder and the dose of calcium chloride. This result indicates a mixed effect of brines on the fatigue performance of the binder.

8. The soaking of all the asphalt binders in 23% NaCl brine caused a general decrease in the stiffnesses, and an increase in the m-values indicated some degree of improvement of the low-temperature properties. The effect of the dose of calcium chloride, in general, decreased the stiffnesses and increased slightly the m-values of the asphalt binders, and again improved their low-temperature properties. Both the creep properties of stiffness and m-value had significant differences caused by the type of binder.
9. Given the range of brine concentrations, higher concentrations (20% and 25% $CaCl_2$) caused more damage in PCC pavement than lower concentrations (0%, 5%, and 10% $CaCl_2$) when concrete was constantly exposed to brine solutions at above-freezing temperatures. On the other hand, concrete samples appeared more prone to freeze–thaw damages at lower concentrations (0% and 5% $CaCl_2$), which was also confirmed with surface scaling and weight loss data.
10. Soaking of asphalt binders in solutions of deicers decreased the Young's modulus and adhesion force regardless of the type of asphalt binders. Furthermore, both Young's modulus and adhesion decreased as the dose of deicers in the solution increased.
11. The epoxy-coated dowel bars were found to be excellent in preventing any corrosion. Type F fly ash was determined to be effective in reducing F–T damages

across the brine concentrations. This favorable effect was further escalated in ambient erosion conditions, especially at 0% $CaCl_2$. At above-freezing temperatures, a bit higher air contents than 6.5% were beneficial for PCC pavement to be resistant to chloride ions, especially at lower concentrations (0% and 5% $CaCl_2$), but air contents too high (12% in this study) would show no benefits.

RECOMMENDATIONS

1. A blended brine with sodium and calcium chlorides can be used when the forecast temperature is below 15°F. The recommended mix ratio of calcium chloride in the blended brine is 15% and should not exceed 20% to avoid clogging the application system. For deicing, blended brine with sodium chloride and calcium chloride can be used at a temperature of 15°F or below. A detailed guideline on material selection and application rate is provided in Appendix A of this report.
2. No significant negative effect has been observed on typical GDOT asphalt binders after soaking in brine solutions. No significant abrasion damage was observed from asphalt concrete with deicing aggregates on the surface. A further research is recommended to study the impact of deicers on the durability of aggregate and the asphalt concrete mixture.
3. The EC dowel bars are found to be excellent in preventing any corrosion. However, the test proposed and conducted in this study lacks some experimental sophistications, mainly due to the limited testing resources. Therefore, a comprehensive research must be designed and conducted to validate the current

findings under a broader spectrum of testing conditions, including W-D cycles at higher temperatures.

4. Type F fly ash would be effective in reducing F–T damages across the brine concentrations. This favorable effect is further escalated in ambient erosion conditions, especially at 0% CaCl2. Therefore, for the future, Type F fly ash can be considered as one of cementitious materials alongside Portland cement for the future concrete pavements.

APPENDIX A. MATERIAL APPLICATION GUIDELINE FOR ANTI-ICING AND DEICING

INTRODUCTION

The purpose of this guideline is to provide recommendations for winter roadway maintenance operations regarding the use of anti-icing and de-icing materials in Georgia. This guideline is largely based on the results from GDOT Research Project 18-28, the FHWA guideline, and a review of other states' practice. This guideline includes recipe of the blends of the liquid and solid chemicals and the applications rate under different winter weather conditions.

ANTI-ICING AND DEICING

Anti-icing refers to pre-treatment operations before the winter event starts. The purpose of anti-icing operations is to prevent the formation of ice bond or the accumulation of snow. Pre-treatment should normally be performed 12-18 hours prior to the onset of the winter event. Applications more than three days before the event should be avoided. If the upcoming winter storm does not start with a heavy rain, liquid application (brine) is usually the most effective. Otherwise, solid application should be considered for anti-icing. Pre-treatment for bridges should be considered for all winter weather events to prevent the formation of black ice.

Deicing refers to post-treatment operations during or after the winter event. The purpose of deicing is to remove the accumulated snow or ice from the road surface and return it to a wet or clear condition quickly. Deicers may be applied in solid, liquid, and a combination

of both forms. Liquid application should be considered if the pavement is dry or when there is a strong wind. Previous GDOT experience that a combined use of solid and liquid application (in two rounds) brings satisfactory result in deicing is also recommended.

PRE-WETTING

Pre-wetting the rock salt before spreading can improve the performance of the salt at lower temperatures. The moisture helps the solid chemicals to bond to the road surface as well as to activate the chemical reaction. Pre-wetting can be done with 23% sodium chloride brine when the forecast temperature is below 25°F (−4°C) or 30% calcium chloride brine when the forecast temperature is below 20°F (−7°C). The mixing rate is usually 6-8 gallon (23-30 L) of brine per ton of rock salts.

BLENDING

Unless combined with other chemicals, sodium chloride is effective only when the temperature is at or above 15°F (−4°C). If the forecast temperature during the event is below 15°F (−9°C), calcium chloride ($CaCl_2$) and sodium chloride can be blended, in either liquid or solid applications.

ABRASIVE

The 89 stone can be used as an abrasive at a ratio of no more than 3:1 (Stone/Salt) when traction is an issue or when snow/ice has accumulated on the roadway.

APPLICATION RATE

The suggested rates for both liquid and solid applications are presented in Table 46 to Table 49. Each table represents a different type of winter weather event. It should be noted the application rate in these tables are the recommended ranges under typical situations. The actual storm type, severity, and duration should be considered by the maintenance engineer when determining the actual application rate.

Table 46. Freezing Rain or Sleet.

Lowest Forecast Pavement Temperature	Anti-Icing (Pretreatment)		De-Icing (During or After the Event)	
	Liquid	Rate* (lb/lm)	Solid	Rate* (lb/lm)
Above 32°F (0°C)	None**	--	None**	--
25 to 32°F (0 to -4°C)	Solid NaCl	40 (11 kg/lkm)	Solid NaCl	40 (11 kg/lkm)
15-25°F (-4 to -9°C)	Solid NaCl	40-80 (11 to 23 kg/lkm)	Solid NaCl	40-100 (11 to 28 kg/lkm)
Below 15°F (-4°C)	Blend of Solid NaCl+$CaCl_2$ (5:1 ratio)	40-80 (11 to 23 kg/lkm)	Blend of Solid NaCl+$CaCl_2$ (5:1 ratio)	40-100 (11 to 28 kg/lkm)

* Application rates may be adjusted by engineer based on the actual storm

** Monitor the temperature carefully for possible drops

Table 47. Frost or Black Ice.

Lowest Forecast road Pavement Temperature	Anti-Icing (Pre-treatment)***				De-Icing (During or After the Event)			
	Road is dry before the freezing temperature		Heavy rain is expected after the pre-treatment		Road is dry with strong wind		Road is wet	
	Liquid	Rate* (gal/lm)	Solid	Rate* (lb/lm)	Liquid	Rate* (gal/lm)	Solid	Rate* (lb/lm)
Above 32°F (0°C)	None**	--	None**	--	None**	--	None**	--
25 to 32°F (0 to -4°C)	23% NaCl Brine	40 (94 L/lkm)	Solid NaCl	40 (11 kg/lkm)	23% NaCl Brine	40 (94 L/lkm)	Solid NaCl	40 (94 L/lkm)
15-25°F (-4 to -9°C)	23% NaCl Brine	40-80 (94-188 L/lkm)	Solid or prewetted solid NaCl	40-80 (11 to 23 kg/lkm)	23% NaCl Brine	40-80 (94-188 L/lkm)	Solid or prewetted solid NaCl	40-100 (11 to 28 kg/lkm)
Below 15°F (-4°C)	Blend of 23% NaCl +30% $CaCl_2$ Brine (5:1 ratio)	40-80 (94-188 L/lkm)	Blend of Solid NaCl+$CaCl_2$ (5:1 ratio)	40-80 (11 to 23 kg/lkm)	Blend of 23% NaCl +30% $CaCl_2$ Brine (5:1 ratio)	40-80 (94-188 L/lkm)	Blend of Solid NaCl+$CaCl_2$ (5:1 ratio)	40-100 (11 to 28 kg/lkm)

* Application rates may be adjusted by engineer based on the actual storm

** Monitor the temperature carefully for possible drops

***Black ice treatment for bridges need to be considered for any winter event.

Table 48. Light snow (falling rate <= than ½" per hour).

Lowest Forecast road Pavement Temperature	Anti-Icing (Pre-treatment)				De-Icing (During or After the Event)			
	Road is dry or slightly wet before the freezing temperature		Heavy rain is before the freezing temperature		Road is icy or with a thin layer of snow		No ice bond below the snow	
	Liquid	Rate* (gal/lm)	Solid	Rate* (lb/lm)	Liquid	Rate* (gal/lm)	Solid	Rate* (lb/lm)
Above 32°F (0°C)	None**	--	None**	--	None**	--	None**	--
25 to 32°F (0 to -4°C)	23% NaCl Brine	40 (94 L/lkm)	Solid NaCl	40 (11 kg/lkm)	23% NaCl Brine	40 (94 L/lkm)	Solid NaCl	40 (11 kg/lkm)
15-25°F (-4 to -9°C)	23% NaCl Brine	40-80 (94-188 L/lkm)	Solid or prewetted solid NaCl	40-100 (11 to 28 kg/lkm)	23% NaCl Brine	40-80 (94-188 L/lkm)	Solid or prewetted solid NaCl	40-200 (11 to 56kg/lkm)
Below 15°F (-4°C)	Blend of 23% NaCl +30% $CaCl_2$ Brine (5:1 ratio)	40-80 (94-188 L/lkm)	Blend of Solid NaCl+$CaCl_2$ (5:1 ratio)	40-100 (11 to 28 kg/lkm)	Blend of 23% NaCl +30% $CaCl_2$ Brine (5:1 ratio)	40-80 (94-188 L/lkm)	Blend of Solid NaCl+$CaCl_2$ (5:1 ratio)	40-200 (11 to 56 kg/lkm)

* Application rates may be adjusted by engineer based on the actual storm

** Monitor the temperature carefully for possible drops

Table 49. Moderate to heavy snow (falling rate > ½" per hour).

Lowest Forecast road Pavement Temperature	Anti-Icing (Pre-treatment)				De-Icing (During or After the Event)			
	Road is dry or slightly wet before the freezing temperature		Heavy rain is before the freezing temperature		Road is icy or with a thin layer of snow		No ice bond below the snow	
	Liquid	Rate* (gal/lm)	Solid	Rate* (lb/lm)	Liquid	Rate* (gal/lm)	Solid	Rate* (lb/lm)
Above 32°F (0°C)	None**	--	None**	--	None**	--	None**	--
25 to 32°F (0 to -4°C)	23% NaCl Brine	40 (94 L/lkm)	Solid NaCl	40 (11 kg/lkm)	23% NaCl Brine	40 (94 L/lkm)	Solid NaCl	40 (11 kg/lkm)
15-25°F (-4 to -9°C)	23% NaCl Brine	40-80 (94-188 L/lkm)	Solid or prewetted solid NaCl	40-200 (11 to 56kg/lkm)	23% NaCl Brine	40-80 (94-188 L/lkm)	Solid or prewetted solid NaCl	100-200 (28 to 56kg/lkm)
Below 15°F (-4°C)	Blend of 23% NaCl +30% $CaCl_2$ Brine (5:1 ratio)	40-80 (94-188 L/lkm)	Blend of Solid NaCl+$CaCl_2$ (5:1 ratio)	40-200 (11 to 56 kg/lkm)	Blend of 23% NaCl +30% $CaCl_2$ Brine (5:1 ratio)	40-80 (94-188 L/lkm)	Blend of Solid NaCl+$CaCl_2$ (5:1 ratio)	100-200 (28 to 56 kg/lkm)

* Application rates may be adjusted by engineer based on the actual storm

** Monitor the temperature carefully for possible drops

GLOSSARY OF TERMS

Black ice. Popular term for a very thin coating of clear, bubble-free, homogeneous ice which forms on a pavement with a temperature at or slightly above 32°F (0°C) when the temperature of the air in contact with the ground is below the freezing-point of water and small slightly supercooled water droplets deposit on the surface and coalesce (flow together) before freezing.

Freezing rain. Supercooled droplets of liquid precipitation falling on a surface whose temperature is below or slightly above freezing, resulting in a hard, slick, generally thick coating of ice commonly called glaze or clear ice. Non-supercooled raindrops falling on a surface whose temperature is well below freezing will also result in glaze.

Frost. Also called hoarfrost. Ice crystals in the form of scales, needles, feathers, or fans deposited on surfaces cooled by radiation or by other processes. The deposit may be composed of drops of dew frozen after deposition and of ice formed directly from water vapor at a temperature below 32°F (0°C) (sublimation).

Sleet. A mixture of rain and of snow which has been partially melted by falling through an atmosphere with a temperature slightly above freezing.

Light snow. Snow falling at the rate of less than 1/2 in (12 mm) per hour; visibility is not affected adversely.

Moderate or heavy snow. Snow falling at a rate of 1/2 in (12 mm) per hour or greater; visibility may be reduced.

REFERENCES

1. Blackburn, R. R., Bauer, K. M., Amsler, Sr., D. E., Boselly, S. E., and McElroy, A. D. (2004). *Snow and Ice Control: Guidelines for Materials and Methods*. Washington, DC: The National Academies Press. https://doi.org/10.17226/13776.

2. Boselly, S. E. (2008). *Update of the AASHTO Guide for Snow and Ice Control*. NCHRP Project 20-7. Transportation Research Board, Washington, D.C.

3. Ketcham, S. A., Minsk, L. D., Blackburn, R. R., and Fleege, E. J. (1996). *Manual of Practice for an Effective Anti-icing Program: A Guide for Highway Winter Maintenance Personnel*. Report No. FHWA-RD-95-202, Washington, D.C.

4. Washington DOT (2018), *Statewide Snow and Ice Plan*, Obtained from: https://www.wsdot.com/winter/files/SnowIcePlanIntro.pdf, last accessed Dec 23, 2020.

5. Fay, L., Shi, X., and Huang, J. (2013). *Strategies to Mitigate the Impacts of Chloride Roadway Deicers on the Natural Environment*. NCHRP Synthesis 449, Transportation Research Board, Washington, D.C.

6. Hassan, Y., El Halim, A. O., Razaqpur, A. G., Bekheet, W., and Farha, M. H. (2002). "Effects of runway deicers on pavement materials and mixes: Comparison with road salt." *Journal of Transportation Engineering*, 128(4), 385-391.

7. Hoffmann, D. W. (1984). "Changes in structure and chemistry of cement mortars stressed by a sodium chloride solution." *Cement and Concrete Research*, 14(1), 49–56.

8. Hobbs, D. W. (2001). "Concrete deterioration: causes, diagnosis, and minimising risk." *International Materials Reviews*, Taylor & Francis, 46(3), 117–144.

9. Marchand, J., Sellevold, E. J., and Pigeon, M. (1994). "Deicer Salt Scaling Deterioration--An Overview." *ACI Symposium Paper*, 145, 1–46.

10. Sumsion, E. S., and Guthrie, W. S. (2013). *Physical and Chemical Effects of Deicers on Concrete Pavement: Literature Review*. Report No. UT-13.09, Utah Department of Transportation, UT.

11. ASTM D1177. (2017). "Test Method for Freezing Point of Aqueous Engine Coolants." ASTM International, West Conshohocken, PA.

12. Darwin, D., de Noyelles, F. G., and Locke, C. E. (1992). *Handbook of Test Methods for Evaluating Chemical Deicers*. Strategic Highway Research Program, National Research Council, Washington, D.C.

13. ASTM D7552. (2014). "Standard Test Method for Determining the Complex Shear Modulus (G*) Of Bituminous Mixtures Using Dynamic Shear Rheometer." ASTM International, West Conshohocken, PA.

14. ASTM D2872. (2019). "Standard Test Method for Effect of Heat and Air on a Moving Film of Asphalt (Rolling Thin-Film Oven Test)." ASTM International, West Conshohocken, PA.

15. ASTM D6521. (2020). "Standard Practice for Accelerated Aging of Asphalt Binder Using a Pressurized Aging Vessel (PAV)." ASTM International, West Conshohocken, PA.

16. ASTM D6648. (2016). "Standard Test Method for Determining the Flexural Creep Stiffness of Asphalt Binder Using the Bending Beam Rheometer (BBR)." ASTM International, West Conshohocken, PA.

17. Pawel hermanowicz. (2020). *AtomicJ 2.20 Software Manual*. Obtained from: https:// sourceforge.net/projects/jrobust/, last accessed Dec 23, 2020.

18. Nanosurf (2020). *ANA Control and Analysis Software Manual*. Obtained from https:// www.nanosurf.com/en/software/ana-control-and-analysis-software, last accessed Dec 23, 2020.

19. ASTM C150. (2020). "Specification for Portland Cement." ASTM International, West Conshohocken, PA.

20. ASTM C136. (2019). "Test Method for Sieve Analysis of Fine and Coarse Aggregates." ASTM International, West Conshohocken, PA.

21. ASTM C127. (2015). "Test Method for Relative Density (Specific Gravity) and Absorption of Coarse Aggregate." ASTM International, West Conshohocken, PA.

22. ASTM C29. (2017). "Test Method for Bulk Density (Unit Weight) and Voids in Aggregate." ASTM International, West Conshohocken, PA.

23. ASTM C128. (2015). "Test Method for Relative Density (Specific Gravity) and Absorption of Fine Aggregate." ASTM International, West Conshohocken, PA.

24. ASTM C618. (2019). "Specification for Coal Fly Ash and Raw or Calcined Natural Pozzolan for Use in Concrete." ASTM International, West Conshohocken, PA.

25. ASTM C143. (2020). "Test Method for Slump of Hydraulic-Cement Concrete." ASTM International, West Conshohocken, PA.

26. ASTM C231. (2017). "Test Method for Air Content of Freshly Mixed Concrete by the Pressure Method." ASTM International, West Conshohocken, PA.

27. ASTM C39. (2020). "Test Method for Compressive Strength of Cylindrical Concrete Specimens." ASTM International, West Conshohocken, PA.

28. ACI 201.2-16. (2016). *Guide to durable concrete*. American Concrete Institute, Farmington Hills, ML.

29. ACI 211.1-91 (1991). *Standard Practice for Selecting Proportions for Normal Heavyweight, and Mass Concrete*. American Concrete Institute, Farmington Hills, ML.

30. ASTM C192. (2019). "Practice for Making and Curing Concrete Test Specimens in the Laboratory." ASTM International, West Conshohocken, PA.

31. AASHTO M254 (2006), "Standard Specifications for Corrosion-Resistant Coated Dowel Bars." American Association of State Highway and Transportation Officials.

32. Morris, W., Moreno, E. I., and Sagüés, A. A. (1996). "Practical evaluation of resistivity of concrete in test cylinders using a Wenner array probe." *Cement and Concrete Research*, 26(12), 1779–1787.
33. AASHTO TP 95 (2011), "Standard Method of Test for Surface Resistivity of Concrete's Ability to Resist Chloride Ion Penetration." American Association of State Highway and Transportation Officials.

34. ASTM C1556. (2016). "Test Method for Determining the Apparent Chloride Diffusion Coefficient of Cementitious Mixtures by Bulk Diffusion." ASTM International, West Conshohocken, PA.

35. Kessler, R. J., Powers, R. G., Vivas, E., Paredes, M. A., and Virmani, Y. P. (2008). "Surface Resistivity as an Indicator of Concrete Chloride Penetration Resistance." presented at the 2008 Concrete Bridge Conference. St. Louis, MO.

36. Vivas, E., Boyd, A. J., Hamilton III, H. R., and Bergin, M. (2007). *Permeability of Concrete — Comparison of Conductivity and Diffusion Methods*. Report Number 49104504992-12(00026899). University of Florida, Gainesville, FL.

37. Rupnow, T. D., and Icenogle, P. (2011). *Evaluation of Surface Resistivity Measurements as an Alternative to the Rapid Chloride Permeability Test for Quality Assurance and Acceptance*. Report No. FHWA/LA.11/479, Louisiana Transportation Research Center, Baton Rouge, LA.

38. Presuel-Moreno, F., Suares, A., and Liu, Y. (2010). *Characterization of New and Old Concrete Structures Using Surface Resistivity Measurements*. Florida Atlantic University, Dania Beach, FL.

39. Andrade, C., Alonso, C., and Goni, S. (1993). "Possibilities for electrical resistivity to universally characterize mass transport processes in Concrete." *Economic and Durable Construction Through Excellence*, 2(23), 127–134.

40. ASTM C666. (2015). "Test Method for Resistance of Concrete to Rapid Freezing and Thawing." ASTM International, West Conshohocken, PA.

41. ASTM C215. (2019). "Test Method for Fundamental Transverse, Longitudinal, and Torsional Resonant Frequencies of Concrete Specimens." ASTM International, West Conshohocken, PA.

42. Zwillinger, D. and Kokoska, S. (2000). *CRC Standard Mathematical Tables and Formulas*. Chapman and Hall/CRC.

43. Lee, S. K. (2018). *Laboratory Evaluation of Corrosion Resistance of Various Metallic Dowel Bars*. Report No. FHWA-HRT-15-079, Washington, DC., 94.